UNIVERSITY OF HELSINKI REPORT SERIES IN PHYSICS

HU-P-D152

Dimensional Reduction Near the Deconfinement Transition

ALEKSI KURKELA

Division of Elementary Particle Physics
Department of Physics
Faculty of Science
University of Helsinki
Helsinki, Finland

ACADEMIC DISSERTATION
To be presented, with the permission of the Faculty of Science of the University of Helsinki, for public criticism in the Auditorium (A129) of Chemicum, A.I.Virtasen aukio 1, on 16 May 2008, at 12 o'clock.

Helsinki 2008

Cover picture:
Juhani Tuominen

ISBN 978-952-10-3932-4
ISSN 0356-0961
ISBN 978-952-10-3933-1 (pdf-version)
http://ethesis.helsinki.fi
Yliopistopaino
Helsinki 2008

Preface

This thesis is based on research carried out at the Theoretical Physics division of the Department of Physical Sciences in the University of Helsinki. The work was financially supported by the Academy of Finland, contract numbers 104382 and 109720, EU I3 Activity RII3-CT-2004-506078, and foundations of Jenny and Antti Wihuri and Magnus Ehrnrooth.

Most of all, I thank my supervisor Keijo Kajantie, to whom I am very grateful for his guidance and counsel. I am also indebted to the referees of this thesis, Mikko Laine and Kari Rummukainen. I express my gratitude towards Kari Rummukainen, from whom I have learned the art of lattice simulations and who has offered his invaluable advice to me on numerous occasions. I am grateful for Mikko Laine for his critical and accurate comments during the period of my graduate studies, from which I have significantly benefited. I also thank York Schröder for tutoring in FORM.

During the two years of my graduate studies, I have been privileged to collaborate with Ari Hietanen, Philippe de Forcrand and Aleksi Vuorinen. I thank Ari Hietanen for numerous enjoyable conversations, as well as for a successful collaboration. I also thank Philippe de Forcrand for a pleasant collaboration. A very special thanks goes to Aleksi Vuorinen who has as a senior colleague tutored me during my studies, often read through and commented my texts and encouraged me in my work.

I also thank my friends and colleagues at the department Antti Gynther, Matti Järvinen, Reijo Keskitalo, Sami Nurmi, Olli Taanila, Heikki Ristolainen, and Mikko Vepsäläinen (certainly including A. H. and A. V.) and many others for physics related discussions, but even more for many entertaining carousals.

Last, I thank my family for support and example.

Helsinki, April 2008

Aleksi Kurkela

A. Kurkela: Dimensional Reduction Near the Deconfinement Transition, University of Helsinki, 2008, 46 p. + appendices, University of Helsinki, Report Series in Physics, HU-P-D152, ISSN 0356-0961, ISBN 978-952-10-3932-4 (printed version), ISBN 978-952-3933-1 (pdf version).
INSPEC classification: A0570, A1110, A1130J, A1235C, A1240E.
Keywords: quantum chromodynamics, quark-gluon plasma, finite-temperature field theory, effective field theory, lattice field theory.

Abstract

When ordinary nuclear matter is heated to a high temperature of $\sim 10^{12}$K, it undergoes a deconfinement transition to a new phase, strongly interacting quark-gluon plasma. While the color charged fundamental constituents of the nuclei, the quarks and gluons, are at low temperatures permanently confined inside color neutral hadrons, in the plasma the color degrees of freedom become dominant over nuclear, rather than merely nucleonic, volumes.

Quantum Chromodynamics (QCD) is the accepted theory of the strong interactions, and confines quarks and gluons inside hadrons. The theory was formulated in early seventies, but deriving first principles predictions from it still remains a challenge, and novel methods of studying it are needed. One such method is dimensional reduction, in which the high temperature dynamics of static observables of the full four-dimensional theory are described using a simpler three-dimensional effective theory, having only the static modes of the various fields as its degrees of freedom.

A perturbatively constructed effective theory is known to provide a good description of the plasma at high temperatures, where asymptotic freedom makes the gauge coupling small. In addition to this, numerical lattice simulations have, however, shown that the perturbatively constructed theory gives a surprisingly good description of the plasma all the way down to temperatures a few times the transition temperature. Near the critical temperature, the effective theory, however, ceases to give a valid description of the physics, since it fails to respect the approximate center symmetry of the full theory. The symmetry plays a key role in the dynamics near the phase transition, and thus one expects that the regime of validity of the dimensionally reduced theories can be significantly extended towards the deconfinement transition by incorporating the center symmetry in them.

In the introductory part of the thesis, the status of dimensionally reduced effective theories of high temperature QCD is reviewed, placing emphasis on the phase structure of the theories. In the first research paper included in the thesis, the non-perturbative input required in computing the $\mathcal{O}(g^6)$ term in the weak coupling expansion of the pressure of QCD is computed in the effective theory framework at an arbitrary number of colors N_c. The two last papers on the other hand focus on the construction of the center-symmetric effective theories, and subsequently the first non-perturbative studies of these theories are presented. Non-perturbative lattice simulations of a center-symmetric effective theory for SU(2) Yang-Mills theory show — in sharp contrast to the perturbative setup — that the effective theory accommodates a phase transition in the correct universality class of the full theory. This transition is seen to take place at a value of the effective theory coupling constant that is consistent with the full theory coupling at the critical temperature.

Contents

List of included papers

The three articles included in this thesis are [1, 2, 3]:

- A. Hietanen and A. Kurkela,
  "Plaquette expectation value and lattice free energy of three-dimensional SU(N_c) gauge theory,"
  JHEP **0611** (2006) 060 [hep-lat/0609015].

- A. Kurkela,
  "Framework for non-perturbative analysis of a Z(3)-symmetric effective theory of finite temperature QCD,"
  Phys. Rev. D **76** (2007) 094507 [arXiv:0704.1416 [hep-lat]].

- Ph. de Forcrand, A. Kurkela and A. Vuorinen,
  "Center-Symmetric Effective Theory for High-Temperature SU(2) Yang-Mills Theory,"
  arXiv:0801.1566 [hep-ph].

The first paper is a result of joint collaboration and both authors contributed at all stages of the work.

In the last paper, the present author constructed the effective theory in collaboration with A. Vuorinen based on an idea by Ph. de Forcrand. The computation of the effective potential and the matching to the 4d theory was independently carried out by the present author and A. Vuorinen. The present author formulated the theory on a lattice and performed the two-loop lattice perturbation theory computations required for the matching between the lattice and the continuum theories. The author wrote the simulation code and performed the numerical part of the work, a part of which was independently verified by Ph. de Forcrand. The paper was written jointly by the collaborators.

Chapter 1

Introduction

Quantum Chromodynamics (QCD), the theory of strong interactions, predicts that ordinary nuclear matter, when heated to a high temperature of $T_c \sim 10^{12}$K, melts to a plasma of strongly interacting quarks and gluons. Traces of this novel matter have been seen in experiments at Relativistic Heavy Ion Collider (RHIC) in the Brookhaven National Laboratory (BNL), where in the most central Au+Au collisions at the highest beam energy, evidence has been found for the formation of a very high energy density system whose description in terms of simple hadronic degrees of freedom is inappropriate [4]. Similar experiments will start soon in LHC at CERN and in FAIR at GSI Darmstadt. In order to gain understanding about the phenomena present in the heavy ion collisions, it is necessary to theoretically understand the thermodynamical properties of quark-gluon plasma.

Non-perturbative lattice simulations provide in principle a conclusive method for studying the equilibrium thermodynamics of the plasma at zero chemical potential [5, 6, 7, 8]. However, technical difficulties persist. The difficulty there is to control the extrapolation to the continuum limit $a \to 0$, as finite temperature imposes additional challenges compared to the $T = 0$ case. Near the crossover regime, the fluctuations are enhanced leading to the requirement of much higher statistics for similar accuracy. This forces a compromise on the lattice spacing, which at present is often 2-3 times larger than for $T = 0$. At higher temperatures $T > T_c$, fluctuations are reduced but now one encounters a large scale difference between the hadronic scale ~ 1 fm and the scale set by the inverse temperature $1/T$. The lattice spacing must be further reduced to satisfy $a \ll 1/T$ while preserving a spatial extent of $\mathcal{O}(2)$ fm.

The latter technical problem can be turned to an advantage by performing one more analytic step before discretizing the theory, namely dimensional reduction [9, 10]. By Fourier-expanding the 4d fields along the Euclidean time direction of extent $1/T$, it can be seen that the non-static modes have energy $\sim \pi T$, and are much heavier than the static modes which have energy gT (soft electric modes) or g^2T (ultra-soft magnetic modes). At high T, the hard modes can be integrated out analytically, resulting in an effective three dimensional (3d) theory of the static modes A_i and A_0 called Electrostatic QCD (EQCD), in which the effect of the non-static hard modes is absorbed in the effective couplings of the theory. From the computational point of view, this brings an additional significant benefit, as the quark sector, the main nuisance in the full theory simulations, does not contain static modes and is integrated out completely in the reduction procedure. The parameters of the dimensionally reduced theory are fixed so that the Green's functions, at large distances $\gg 1/T$, coincide with those of the original 4d theory. At high temperature,

asymptotic freedom makes $g(T)$ small and this matching of coefficients can be performed analytically in continuum perturbation theory. The expansion parameter in the matching is actually $N_c g^2(T)/(4\pi)^2$ rather than just $g^2(T)$ allowing the series to convergence quite fast even at lower temperatures where g is not so small. Moreover, the optimal scale for the running of g, for which the high order contributions are minimized, is $\sim 7T$ rather than $\sim T$, giving a boost for the convergence especially near T_c [11]. At that stage, the 3d theory is discretized and can be simulated on a fine grid with a moderate computing effort [12, 13, 14, 15, 16].

On the analytic side, this program of dimensional reduction has been pursued for a long time, culminating recently in a calculation of the pressure of the full theory to order $g^6 \log 1/g$ [17, 18, 19], beyond which the diagrammatic expansion fails. In order to evaluate the contributions starting from the next g^6 order, an infinite number of diagrams having different non-trivial topologies and containing arbitrary number of loops would need to be resummed [20]. However, at very high temperature, deep in the perturbative regime, also the color-electric modes can be integrated out resulting in a pure gauge theory in three dimensions, Magnetostatic QCD (MQCD) [9]. Simulations in this three-dimensional theory provide a way to perform the resummation. The first of the papers [1] included in this thesis deals directly with this question. In the paper, the plaquette expectation value of three-dimensional pure gauge theory is measured on the lattice for an arbitrary number of colors (N_c), providing the only part for the g^6 coefficient of the pressure not attainable by analytic calculations.

Non-perturbative simulations in EQCD have produced results matching those of the 4d theory at high temperature [21], but also surprisingly close to T_c down to $\sim 2T_c$ [14, 15]. However, EQCD fails to capture the approach to the deconfinement transition at T_c. This comes as no surprise as the dynamics responsible for the qualitative change at T_c, namely the $\mathrm{Z}(N_c)$ center symmetry of 4d Yang-Mills theory, is not accommodated in the theory. Because of the perturbative construction of EQCD, it only deals with small fluctuations around the $A_0 = 0$ vacuum, totally ignoring the other $\mathrm{Z}(N_c)$ vacua of the 4d theory, where the color-electric field gets values $\sim T/g$. This gives the motivation for incorporating the center symmetry in the 3d theory. The improvement should extend the range of validity of dimensional reduction downwards in temperature, hopefully all the way to the non-perturbative regime near T_c.

The second and third of the papers included in this thesis [2, 3] discuss dimensionally reduced effective theories which respect the center symmetry. Such a theory for coarse-grained Wilson lines in SU(3) Yang-Mills theory was introduced in Ref. [23] and was formulated on a lattice in Ref. [2] for non-perturbative study. The superrenormalizability of the theory allows to match the lattice and continuum theories exactly in g for a fine lattice spacing. The matching requires two-loop lattice perturbation theory calculations, performed in Ref.[2], allowing to simulate the theory with physical continuum parameters. As a first step in the non-perturbative study of the theory, a subset of the phase diagram of the theory was determined using numerical lattice simulations. In the case of SU(3), however, the parameter space of the theory is very large, making the matching of the parameters difficult, and for simplicity, a large (but motivated) set of operators was discarded in the construction of the theory. Even with the reduced set of operators, the large parameter space renders simulations of the theory quite demanding.

In Ref. [3] a corresponding theory for SU(2) gauge theory was constructed to create a more economical platform to study the significance of the center symmetry. The simpler

structure of the SU(2) gauge group leads to a markedly simpler effective theory, and the simulations are less time consuming. In Ref. [3], the theory was formulated both in the continuum and on the lattice including exact lattice-continuum matching. The parameters of the effective theory were matched to full theory to the leading order in continuum perturbation theory.

The phase diagram of the effective theory was determined using non-perturbative lattice simulations. In semi-classical approximation, the phase diagram was observed to be trivial: the theory lies always in the symmetric phase. However, non-perturbative effects dynamically generate a second order phase transition, which is in the same universality class as the 4d theory transition [24]. This is a direct consequence of the effective theory respecting all the symmetries of the full theory, and the behavior is in sharp contrast to that of center symmetry breaking effective theories and strongly encourages further studies.

The ability to correctly describe the phase transition should be put to test in the future. Particularly interesting will be the inclusion of quarks to the theory: The effect of quarks will be described by new operators breaking the center symmetry softly and will fundamentally modify the dynamics near T_c. If the effective theory can accommodate the correct phase transition as in the SU(2) quarkless case, it would provide a great laboratory to investigate finite-temperature massless QCD, at a computer cost negligible compared to full-fledged QCD simulations. Also, the quark number chemical potential (μ) can be incorporated in the theory, and should the correct phase transition dynamics persist, it can act as a unique platform to study the possible critical point in the $T - \mu$ plane.

This thesis is organized as follows. In Chapter 2, some generic features of Quantum Chromodynamics at finite temperature are discussed, some results from the literature relevant to the topic are reviewed, and the theoretical framework for dimensional reduction is presented. The center symmetry breaking dimensionally reduced theories Electrostatic QCD (EQCD) and Magnetostatic QCD (MQCD) are introduced, giving special attention to the phase diagram of the former in order to provide a point of comparison for the center symmetric theories. Also, the computation of the pressure of full QCD to g^6 using EQCD and MQCD is discussed and the main results of simulations of Ref. [1] are presented. In Chapter 4, the construction of center symmetric effective theories is reviewed, and the current understanding is summarized. Review and outlook are given in Chapter 5.

Chapter 2

Thermodynamics of QCD

In this Chapter, a brief introduction to equilibrium thermodynamical properties of QCD at finite temperature is presented. The introduction is not meant to be a comprehensive one but to depict the physical situation for subsequent discussions. The theoretical formulation of quantum fields at finite temperature is discussed and the Lagrangian of QCD is presented, giving special attention to the center symmetry and the related order parameter, the Polyakov loop. The notion of dimensional reduction is presented in detail.

2.1 Physics of strong interactions at finite temperature

Lattice simulations at zero baryon number chemical potential have been able to establish that there exist two phases, which have very different quantitative properties in strongly interacting matter in thermal equilibrium [7]. At low temperature the matter consists of massive hadrons, but as the temperature is increased, there is a rapid liberation of the partonic degrees of freedom and the matter enters the deconfined phase. The simulations have demonstrated that the transition from the confined phase to the deconfined phase is not a singular phase transition, but rather a broad cross-over. Since the transition is non-singular, different observables lead to different numerical values of the critical temperature T_c. In Ref. [8] the value obtained from the maximum of the chiral susceptibility is $T_c = 151(4)$MeV whereas the critical temperature defined through the behavior of the Polyakov loop gives a value $T_c = 176(6)$MeV, depicting the broad nature of the cross-over.

The order of the transition depends on quark masses. A schematic phase diagram of the theory as a function of the strange quark mass and the degenerate mass of light up and down quarks from Ref. [25] is shown in Fig. 2.1. In the limit of infinitely heavy quarks, the quarks decouple and the resulting action has a global $\mathrm{Z}(N_\mathrm{c})$ center symmetry and an order parameter, the Polyakov loop, rendering a genuine first order transition. For the two color case of SU(2), the theory on the other hand has a continuous second order phase transition in this limit. In a similar fashion, in the limit of vanishing quark masses the system has a global chiral symmetry and the transition is again of first order. Finite quark masses break both symmetries allowing regions of first order transition and cross-over separated by second order transition lines in the 3d Ising universality class. The physical quark masses lie in the cross-over region [7]. In the chiral limit of two-flavor QCD, corresponding to an infinite strange quark mass, the transition is of second order, with a universality class that has not yet been definitely identified.

The equation of state near T_c (with a so called staggered fermion p4-action at $N_t = 4$,

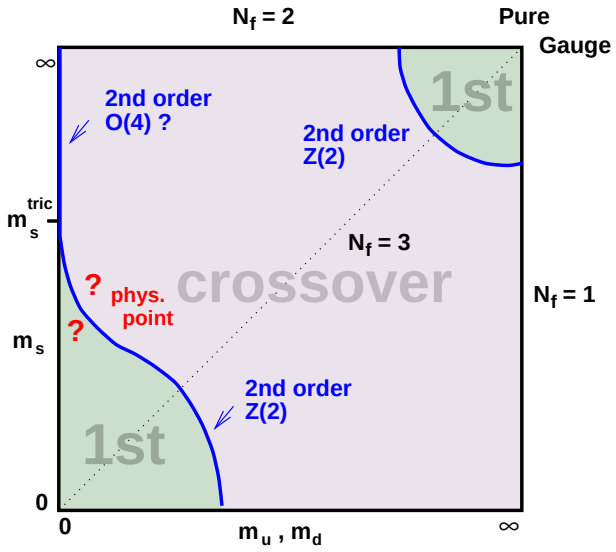

Figure 2.1: A schematic phase diagram of QCD in the plane of strange and degenerate up and down quark masses taken from Ref. [25]. In the infinite quark mass limit, the center symmetry provides an order parameter and the phase transition of first order. At vanishing quark masses, there is a global symmetry, the chiral symmetry and the transition is again of first order. Lattice simulations show that between these two regimes of first order transition, the transition turns to a cross-over and the cross-over region is separated from the first order transitions by second order transition lines. The physical point lies most probably in the cross-over region.

with a light quark mass $m/T = 0.4$ and a heavy quark mass $m/T = 1$) from [26] is displayed in Fig. 2.2. The behavior of the equation of state can be analytically understood in both the low and high temperature limits. Below the critical temperature, the thermodynamic properties of QCD can be phenomenologically modeled as those of a non-interacting gas of hadron resonances [27]. The strong interactions of the partons are implicitly included in the model in the form of the resonances. The comparison of the predictions of the resonance gas model with the lattice data from Ref. [28] is shown in Fig. 2.3. The model includes all the mesonic and baryonic resonances up 1.8 GeV and 2.0 GeV amounting to 1026 resonances. The energy density rises rapidly just below the critical temperature as there is an increasing number of effective degrees of freedom available. The model fails to give a good description at high temperature where the hadrons, extended objects with a typical size $\sim$1 fm, start to overlap.

At asymptotically high temperature, the interactions between partons become weak [29] and the plasma is described by a free gas of quarks and gluons. As seen from Fig. 2.2, however, the convergence towards the Stefan-Boltzmann limit is very slow: At $T \approx 3.5T_c$ the pressure is only $\sim$ 80% of the non-interacting limit, signalling that interactions are still present in the plasma. The picture of a free parton gas can be refined by considering interactions in perturbation theory, in which the equation of state has been calculated up to and including the $\mathcal{O}(g^5)$ term [30]. In addition, the coefficient of $g^6 \log g$ is known [12], but it does not constitute a unique term to the series until the $\mathcal{O}(g^6)$ term is evaluated. The convergence of the weak coupling expansion is slow even at very high temperatures

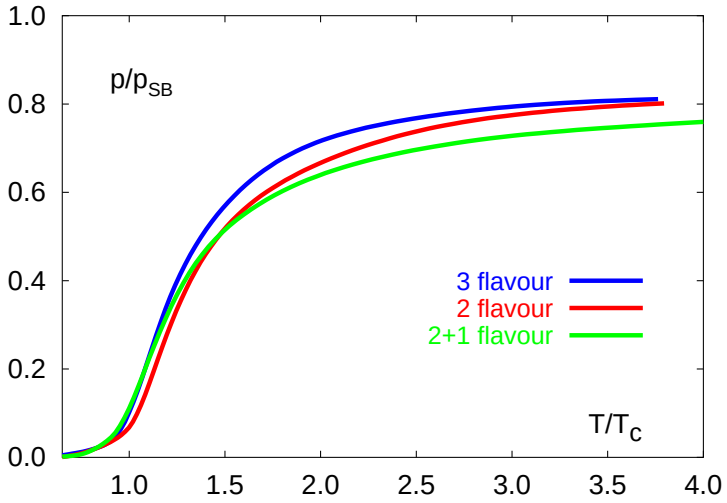

Figure 2.2: Equation of state of QCD from [26] with two and three light quarks and with two light and one heavy quark with staggered p4-action at $N_t = 4$, the mass of the light quarks being $m/T = 0.4$ and for the additional heavy quark $m/T = 1$. The pseudo-critical temperature is defined to be the maximum of the Polyakov loop susceptibility.

(see Fig. 2.4): For example, even at $T = 10^6 T_c$, the g^5 term gives a larger contribution to the pressure than the g^4 term [12, 31].

It is noteworthy that thermodynamical quantities, such as the pressure, interaction measure and energy density, are proportional to the power of temperature naively given by their mass dimension in arbitrary order of the weak coupling expansion up to logarithmic corrections. For example, the weak coupling expansion gives for the interaction measure

$$\epsilon - 3p(T) \quad \approx \quad f_{\text{pert}}(T) T^4, \tag{2.1}$$

where the temperature dependence of the dimensionless coefficient $f_{\text{pert}}(T)$ is logarithmic. However, lattice data seems to indicate that up to temperatures a few times the critical temperature, the dominant power-like behavior is rather $\mathcal{O}(T^2)$ than $\mathcal{O}(T^4)$ (see Fig. 2.5), and the thermodynamical observables are better described by the phenomenological ansatz [32, 33]

$$\epsilon - 3p(T) \quad \approx \quad f_{\text{pert}}(T) T^4 + bT^2 + c. \tag{2.2}$$

where the contributions attainable from perturbation theory determine only the leading high temperature behavior. This kind of power behavior may arise quite naturally from the extensions of the MIT bag model and from gauge-gravity duality considerations [32, 34].

2.2 Path integral

A convenient way to describe the state of any statistical quantum mechanical system is in terms of its density operator

$$\rho = \sum_i p_i |\Psi_i\rangle\langle\Psi_i|, \tag{2.3}$$

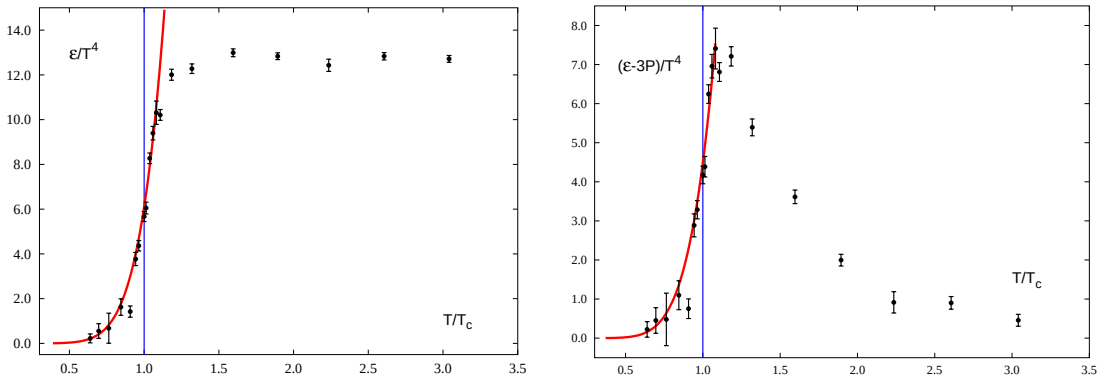

Figure 2.3: Comparison of the predictions of the resonance gas model and lattice QCD from Ref. [28]. The left panel shows the energy density ϵ in units of T^4 with (2+1) quark flavors as a function of T/T_c. On the right panel, the corresponding results are shown for the interaction measure $(\epsilon - 3p)/T^4$. The solid lines are results from the hadron resonance gas model.

where the probability of the system being in the state $|\Psi_i\rangle$ is given by p_i. The system is in thermal equilibrium, if its macroscopic observables are constants in time and at the same time the entropy of the system is maximized respecting the bounds given by the macroscopical observables. The density operator of such an equilibrium system with fixed average energy is the Boltzmann operator

$$\rho = \exp(-\beta \hat{H}), \tag{2.4}$$

where $\hat{H}$ is the Hamiltonian of system and β is the Lagrange multiplier identified with the temperature through $\beta = 1/k_B T$.

The thermal average of any operator $\mathcal{A}$ is then defined as

$$\langle \mathcal{A} \rangle = \frac{1}{Z} \mathrm{Tr}\, \rho \mathcal{A}, \tag{2.5}$$

where Z is the partition function of the system

$$Z(T, V) = \mathrm{Tr}\, \rho = \mathrm{Tr}\, \exp(-\beta \hat{H}) = \sum_i \langle \phi_i | e^{-\beta \hat{H}} | \phi_i \rangle, \tag{2.6}$$

with an arbitrary complete orthonormal basis of states $\{|\phi_i\rangle\}$. All the equilibrium thermodynamical information of the system is encoded in the partition function, that is, all thermodynamical quantities are given by the partial derivatives of the partition function. The most fundamental of them, the pressure, entropy, and internal energy read

$$p = T \frac{\partial \log Z}{\partial V}, \qquad S = T \frac{\partial \log Z}{\partial T}, \tag{2.7}$$

and

$$E = -pV + TS. \tag{2.8}$$

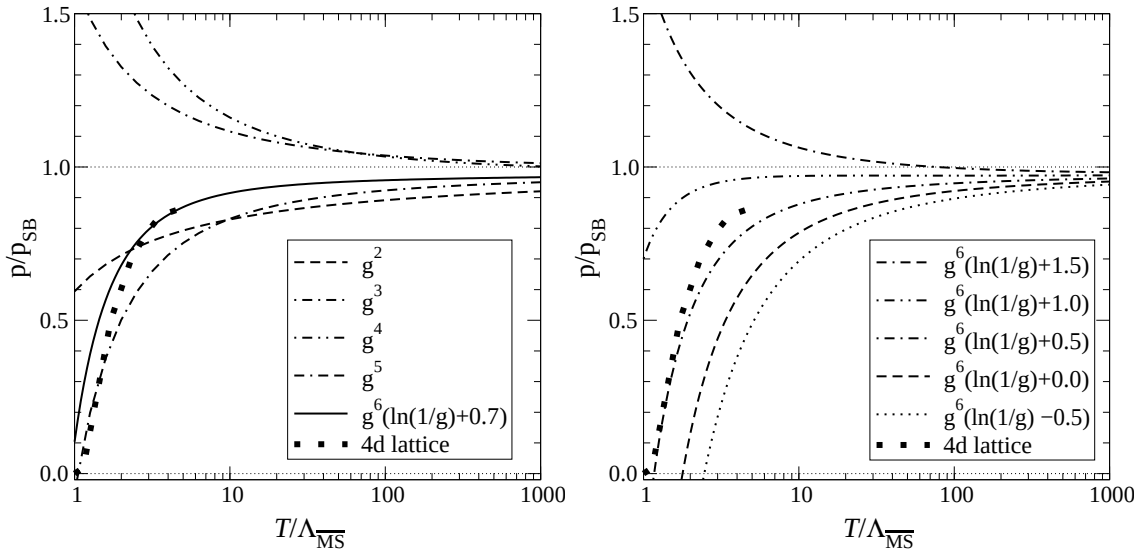

Figure 2.4: On the left panel, results of the weak coupling expansion (with no fermions) at various orders in the renormalized coupling g as taken from Ref. [17]. The unknown coefficient of the g^6 term is dialed to give the best possible fit with the lattice data. On the right panel, the dependence on the missing coefficient of g^6.

In the context of quantum field theories, a very useful way of expressing the partition function is the path integral formulation. We can interpret the operator $e^{-\beta\hat{H}}$ as translating a state to an imaginary time direction $t = -i\beta$ and can readily write the corresponding transition amplitude (in $d+1$ dimensions)

$$\langle\phi_2|e^{-\beta H}|\phi_1\rangle = \int_{\phi(x,0)=\phi_1}^{\phi(x,\beta)=\phi_2} \mathcal{D}\phi\mathcal{D}\pi \exp(\int_0^\beta \mathrm{d}\tau \int \mathrm{d}^d x \left(i\pi(x,\tau)\dot{\phi}(x,\tau) - H(\pi,\phi)\right), \quad (2.9)$$

where the field $\pi(x,\tau)$ is the canonical conjugate of $\phi(x,\tau)$ and H is the Hamiltonian density. The integral $\mathcal{D}\phi\mathcal{D}\pi$ is taken over all possible field configurations. Restricting to a set of theories having at most a quadratic H in π, the Gaussian integral over the conjugate momenta can be trivially performed. By equating fields at the end points $\tau = 0$ and β and summing over all fields, the partition function can be expressed as an integral over all periodic field configurations

$$Z(T,V) = \int \mathcal{D}\phi \exp\left(-\int_0^\beta \mathrm{d}\tau \int \mathrm{d}^d x\, \mathcal{L}(\phi,\partial_\mu\phi)\right) = \int \mathcal{D}\phi \exp\left(-S\right), \quad (2.10)$$

here $\mathcal{L}$ is the Eulcidean Lagrangian of the system. The above discussion was for bosonic fields and the Fermi statistics is implemented into the path integral by summing over anti-periodic configurations instead of the periodic ones.

In addition to the quantities directly related to the partition function, there are also various interesting spatial, or static, correlators. Even though these quantities may not be directly accessible to experiment, their knowledge provides theoretical information about the relevant dynamical length scales present in the system. The connected correlators fall off exponentially at large spatial separations

$$C(\mathbf{x},\mathbf{y}) \equiv \langle \mathcal{A}_r(\mathbf{x})\mathcal{A}_r(\mathbf{y})\rangle \sim e^{-M|\mathbf{x}-\mathbf{y}|}, \quad (2.11)$$

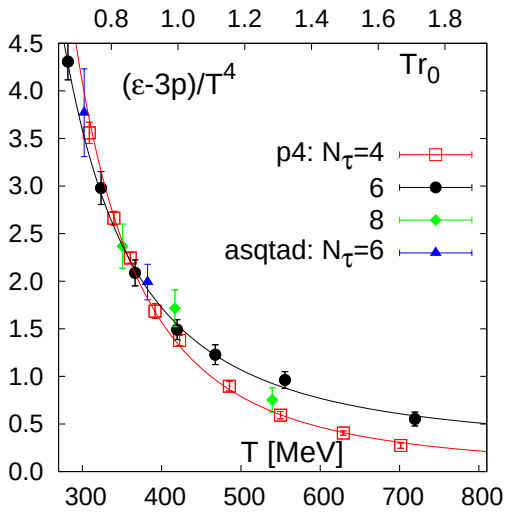

Figure 2.5: The interaction measure as taken from Ref. [33]. At temperatures a few times above the critical temperature, the dominant power like behavior appears to be $\epsilon - 3p \sim T^2$ instead of $\sim T^4$ as predicted by the weak coupling expansion, signalling the presence of non-perturbative physics above the transition temperature. However, the complicated logarithms appearing in the weak-coupling expansion may instate the T^2-behavior.

where $\mathcal{A}$ is an operator constructed from the fields of the theory and r stands for a complete set of quantum numbers. The coefficient M with dimension of mass dictating the exponential fall-off of the spatial correlator is referred to as the screening mass. Because of the shortening of the Euclidean time direction at $T > 0$, the rotation symmetry of the plane orthogonal to the correlation direction is broken down from O(3) to O(2)×Z(2), and the screening masses are classified by the irreducible representations of this group. The physical interpretation of the inverse screening mass corresponds to the scale over which the equilibrated medium is sensitive to a test charge carrying the quantum numbers of the corresponding operator $\mathcal{A}_r$. Beyond the screening length, the medium appears undisturbed.

2.3 Lagrangian of QCD

The partition function of QCD with N_f flavors of quarks with masses m_i and N_c colors in Euclidean signature and in the $\overline{\text{MS}}$ renormalization scheme, is given by

$$Z_{\text{QCD}} = \int \mathcal{D}A_\mu \mathcal{D}\psi \mathcal{D}\bar{\psi}\, e^{-S_{\text{QCD}}}, \tag{2.12}$$

$$S_{\text{QCD}} = \int_0^\beta \mathrm{d}\tau \int \mathrm{d}^d x\, \mathcal{L}_{\text{QCD}}, \tag{2.13}$$

$$\mathcal{L}_{\text{QCD}} = \frac{1}{2}\mathrm{Tr}\, F_{\mu\nu}F_{\mu\nu} + \sum_i^{N_f} \bar{\psi}\left(\gamma_\mu D_\mu + m_i\right)\psi, \tag{2.14}$$

where $\mu, \nu = 0, \ldots, d$. The field strength tensor and the covariant derivative read

$$F_{\mu\nu} = \partial_\mu A_\nu - \partial_\nu A_\mu + ig[A_\mu, A_\nu], \tag{2.15}$$
$$D_\mu = \partial_\mu - igA_\mu. \tag{2.16}$$

The gauge fields A_μ transform in the adjoint representation of the SU(N_c) group and can be expressed using the ${N_\mathrm{c}}^2 - 1$ generators of the group, T^a, as

$$A_\mu = A_\mu^a T^a; \tag{2.17}$$

we assume the normalization $\mathrm{Tr}\, T^a T^b = \frac{1}{2}\delta_{ab}$. The Dirac matrices fulfill the usual relations

$$\gamma_\mu^\dagger = \gamma_\mu \tag{2.18}$$
$$\{\gamma_\mu, \gamma_\nu\} = 2\delta_{\mu\nu} \tag{2.19}$$

The Lagrangian in Eq. (2.13) is invariant under the local gauge symmetry

$$A_\mu \rightarrow \Omega^{-1}(x) A_\mu \Omega(x) + \frac{i}{g}\left(\partial_\mu \Omega^{-1}(x)\right)\Omega(x) \tag{2.20}$$
$$\psi \rightarrow \Omega(x)\psi \tag{2.21}$$

with Ω being an element of the SU(N_c) group.

The action in Eq. (2.13) can also be regularized on a discrete space-time lattice

$$S_{\mathrm{QCD}}^{\mathrm{a}} = \sum_x \mathcal{L}_{\mathrm{QCD}}^{\mathrm{a}}, \tag{2.22}$$

$$\mathcal{L}_{\mathrm{QCD}}^{\mathrm{a}} = \beta \sum_{\mu<\nu}^{4} \left[1 - \frac{1}{N_\mathrm{c}} \mathrm{ReTr}\, P_{\mu\nu}\right] + \sum_x \bar{\psi} K \psi, \tag{2.23}$$

where β is the lattice coupling constant related to the lattice spacing a and $P_{\mu\nu}$ is the plaquette

$$P_{\mu\nu}(x) = U_\mu(x) U_\nu(x + a\hat{e}_\mu) U_\mu^{-1}(x + a\hat{e}_\nu) U_\nu^{-1}(x), \tag{2.24}$$

and U_μ are the link variables, the Wilson lines connecting adjacent sites. The link variables are related to the gauge fields in the continuum theory by a path-ordered integral

$$U_\mu(x) = \mathrm{P} e^{ig \int_x^{x+a\hat{e}_\mu} dy_\nu A_\nu(y)}. \tag{2.25}$$

The discretization of the fermion sector is a very subtle issue [35], and the different choices for fermion matrix K will not be discussed here. The link variables transform under gauge transformations according to their end points

$$U_\mu(x) \longrightarrow \Omega(x) U_\mu(x) \Omega^{-1}(x + a\hat{e}_\mu), \tag{2.26}$$

while the transformation of the fermions is unaltered and is given by Eq. (2.21).

In the absence of quarks, or more precisely any fundamental matter, the Lagrangian has an additional global symmetry. Consider choosing a fixed time slice with $t = t_0$, and then multiplying the link matrices pointing in the Euclidean time direction in the slice by an element of the center of the group $z \in \mathrm{Z}(N_\mathrm{c})$

$$U_0(\mathbf{x}, t_0) \rightarrow z U_0(\mathbf{x}, t_0), \tag{2.27}$$

where we separated explicitly the time coordinate in the argument. The action is obviously invariant under this transformation, with z and z^{-1} canceling in every time-like plaquette at $t = t_0$, as z commutes with all members of the group. For this reason, any other ordinary closed Wilson loop is also invariant under this transformation.

However, there are gauge invariant operators, which do transform non-trivially under Eq. (2.27). Consider a Wilson line which wraps around the periodic Euclidean time direction

$$W(\mathbf{x}) = U_0(\mathbf{x}, 0)U_0(\mathbf{x}, a)U_0(\mathbf{x}, 2a)\dots U_0(\mathbf{x}, 1/T). \tag{2.28}$$

The trace of the thermal Wilson loop

$$L(\mathbf{x}) = \frac{1}{N_\mathrm{c}}\mathrm{Tr}\, W(\mathbf{x}), \tag{2.29}$$

is gauge invariant quantity and is often referred to as the Polyakov loop. Being a trace of a unitary matrix, the Polyakov loop can take values only in a bounded region of the complex plane, as illustrated in Fig. 2.6. Note that for SU(2), the trace of a group member is always real, rendering the Polyakov loop real as well. The Polyakov loop obviously transforms under the $\mathrm{Z}(N_\mathrm{c})$-symmetry in the fundamental representation

$$L(\mathbf{x}) \to zL(\mathbf{x}). \tag{2.30}$$

Therefore a non-vanishing expectation value $\langle L(\mathbf{x})\rangle$ may be taken as a signal for the spontaneous breaking of the global $\mathrm{Z}(N_\mathrm{c})$-symmetry. The Polyakov loop may be interpreted to be related to the free energy F_q of an infinitely heavy isolated test quark

$$\langle L\rangle \sim e^{-F_q(T)/T}, \tag{2.31}$$

and thus it can be used as an order parameter for the deconfinement transition in the absence of dynamical quarks. In the confining phase, the Polyakov loop is identically zero and in the deconfined phase, the Polyakov loop gets a non-zero expectation value. Due to the center symmetry, there are N_c separate but physically equivalent deconfined phases, in which the Polyakov loop takes its value at one of the corners of the bounded area in Fig.(2.6).

The expectation value in fact vanishes for zero lattice spacing, as the renormalization of the operator is not well-defined. However, at any non-zero lattice spacing, it does work as a true order parameter. The operator may be defined also through the asymptotic large distance behavior of static quark-antiquark correlation functions, responsible for the inter-quark potential [5, 6, 36]

$$\langle L\rangle^2 = \lim_{|\mathbf{x}-\mathbf{y}|\to\infty}\langle L(\mathbf{x})L^\dagger(\mathbf{y})\rangle. \tag{2.32}$$

By defining the Polyakov loop using correlators, one thus assures that the operator can be renormalized and has a meaningful continuum limit. This quantity is often referred to as the renormalized Polyakov loop.

When dynamical quarks are present, the $\mathrm{Z}(N_\mathrm{c})$-symmetry is no longer an exact symmetry of the theory allowing the Polyakov loop to deviate from zero. However, the Polyakov loop is close to zero in the confining phase and has a rapid change in the vicinity of the phase transition.

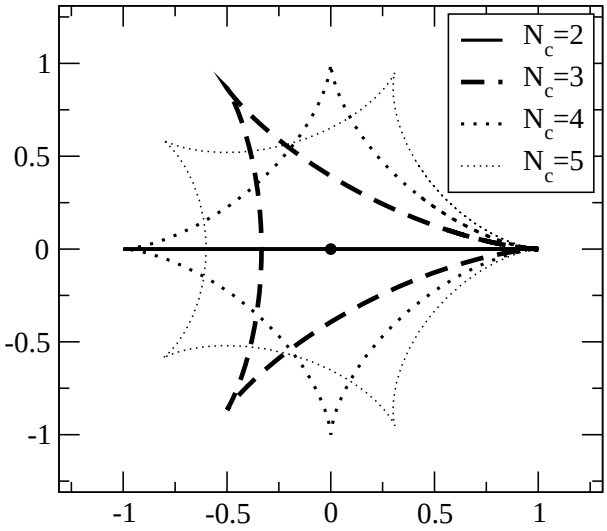

Figure 2.6: The Polyakov loop (for $N_{\rm c} = 2, .., 5$) can take values that lie inside the corresponding graphs. The confining minimum is at the origin and the deconfining minima are at the corners. For the case of $N_c = 2$, the configuration space is reduced to a real line with the deconfining states at the endpoints and the confining vacuum in the middle.

2.4 Effective potential for the Polyakov loop

In the weak coupling expansion, one expands the fields around $A_\mu = 0$, for which $\langle L \rangle = 1$, and assumes that the fluctuations are small. The expansion fails if the fluctuations become large $\mathcal{O}(1/g)$ which is the case when tunneling between the different $N_{\rm c}$ vacua takes place.

It is thus important to find out what is the effective potential of the Polyakov loop at high temperatures. The one-loop effective potential for the Polyakov loop has been calculated in Ref. [37, 38, 39, 40]. . At finite temperature it is not possible to eliminate A_0 totally by going to $A_0 = 0$ gauge, as one does in the $T = 0$ case; such a transformation of the functional integral would force A_i to violate periodic boundary conditions. However, it is possible to fix a gauge where the color-electric field is constant in time and diagonal

$$A_0^{ab}(\mathbf{x}, t) = \frac{\pi T}{g} q_a(\mathbf{x}) \delta_{ab}, \tag{2.33}$$

with the indices being fundamental. The color vector q_a is parametrized as

$$q_a(\mathbf{x}) = \frac{2q(\mathbf{x})}{N_{\rm c}} + 2\tilde{q}_a(\mathbf{x}), \quad a = 1, \ldots, N_{\rm c} - 1, \tag{2.34}$$

$$\sum_a^{N_{\rm c}-1} \tilde{q}_a(\mathbf{x}) = 0 \tag{2.35}$$

$$q_{N_{\rm c}}(\mathbf{x}) = -\frac{N_{\rm c} - 1}{N_{\rm c}} 2q(\mathbf{x}). \tag{2.36}$$

This parametrization is consistent with the constraint that A_0 is traceless. At one-loop level, the effective potential can be split into two parts, one arising from the pure gauge

sector and the other from the quark sector

$$V_{\rm eff}(\tilde{q}_a, q) = V_{\rm eff}^{\rm glue}(\tilde{q}_a, q) + V_{\rm eff}^{\rm fermion}(\tilde{q}_a, q). \tag{2.37}$$

The one-loop effective potential for the purely gluonic part reads

$$V_{\rm eff}^{\rm glue}(\tilde{q}_a, q) \;=\; \frac{2\pi^2 T^4}{3}\left(2\sum_{a=1}^{N_{\rm c}-1} f\left(q-\tilde{q}_a\right) + \sum_{a,b=1}^{N_{\rm c}-1} f\left(\tilde{q}_a-\tilde{q}_b\right)\right), \tag{2.38}$$

with

$$f(q) = [q]^2(1-[q])^2, \quad [q] = |q|_{\rm mod\ 1}\,. \tag{2.39}$$

The effective potential in Eq. (2.38) vanishes for $\tilde{q}_i = 0$ and $q = n$ with $n = 0, 1, \ldots, N_{\rm c}-1$. These $N_{\rm c}$ points are also the global minima. At these minima, the $\mathrm{Z}(N_{\rm c})$ symmetry is manifest in the Polyakov loop

$$L = e^{ig\beta A_0} = e^{2\pi i n/N_{\rm c}}. \tag{2.40}$$

For any other choice of $\tilde{q}_i$ and q, up to a permutation of the diagonal elements, the potential is non-vanishing.

In the presence of $N_{\rm f}$ flavors of massless quarks, the fermion part of the effective potential reads

$$V_{\rm eff}^{\rm fermion}(\tilde{q}_a, q)\Big|_{N_{\rm f}, m_{\rm f}=0} = -N_{\rm f}\frac{4\pi^2 T^4}{3}\left(\sum_{a=1}^{N_{\rm c}-1} f\left(\frac{q}{N_{\rm c}}+\frac{1}{2}+\tilde{q}_a\right) + f\left(\frac{q}{N_{\rm c}}+\frac{1}{2}-q\right)\right) \tag{2.41}$$

The potential arising from the fermions is not periodic in q with period 1 but rather the period is $N_{\rm c}$. This is a manifestation of the broken $\mathrm{Z}(N_{\rm c})$-symmetry. For $\tilde{q}_a = 0$, the fermionic effective potential is minimized for $q = 0$, and the other $\Omega \neq 1$ minima become merely local. At some critical value $N_{\rm f}$, the local minima of the gluonic part are overwhelmed by the fermionic contributions and disappear (see Fig. 2.7).

For massive quarks $m_{\rm f} \neq 0$, the shape of the effective potential depends on the temperature T, even at one-loop level. The effective potential will then be a function of m/T and it will interpolate smoothly between the massless case $m_{\rm f} = 0$ and the $\mathrm{Z}(N_{\rm c})$ symmetric case at $m_{\rm f} \to \infty$.

2.5 Dimensional reduction

In the path integral formalism, the temperature could be interpreted geometrically as the inverse of the extent of the Euclidean time direction. Thus, when one increases the temperature, the time direction shrinks, and if one is interested only in correlators at distances large compared with $1/T$, the system effectively appears to be only three-dimensional. This immediately gives rise to the idea that it should be possible to describe the long distance properties of a high temperature field theory by using a three-dimensional effective field theory. This procedure is known as dimensional reduction [10]. To give a mathematical formulation to the physical idea, consider a Fourier decomposition of the fields along the Euclidean time direction

$$\phi(x) = T\sum_{n=-\infty}^{\infty} e^{i\omega_n t}\phi_n(\mathbf{x}), \tag{2.42}$$

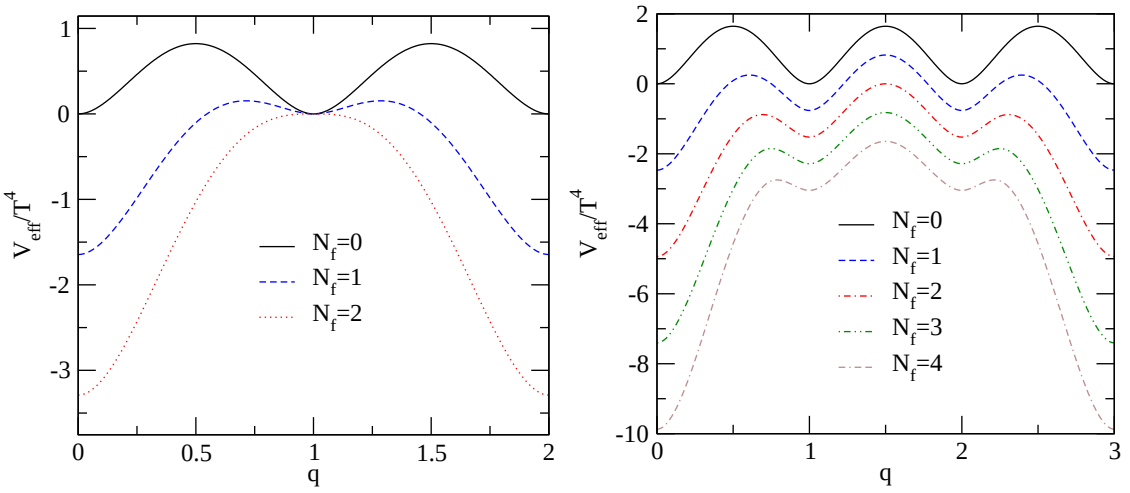

Figure 2.7: The one-loop effective potential of Eq. 2.37 of the Polyakov loop in the cases of gauge group SU(2) (left) and SU(3) (right), with different numbers of massless fermion flavors, parametrized according to Eqs. (2.34)-(2.36).

where the ω_n are the Matsubara modes. The (anti)periodic boundary conditions imply that the corresponding momentum components along this direction are discrete. For the periodic bosons and anti-periodic fermions, it follows that the Matsubara modes are always even for the bosonic fields and odd for the fermionic ones

$$\omega_n = \begin{cases} 2n\pi T & \text{bosons} \\ (2n+1)\pi T & \text{fermions.} \end{cases} \tag{2.43}$$

If the kinetic term has the canonical quadratic form, as is the case of the theories we are interested in, the tree-level propagator (in the massless case) is proportional to $1/(\mathbf{p}^2+\omega_n^2)$. Thus, the Matsubara modes have taken the place of the mass, inducing an effective mass proportional to the temperature for all modes except the static ω_0 mode for the bosons.

At very high temperature, one is tempted to apply the decoupling theorem by Appelquist and Carazzone [41], which states that in renormalizable zero-temperature field theories containing masses with a hierarchy $m_l \ll m_h$, the heavy masses decouple from the physics of the low energy scale of the theory, where the typical momentum scale is $|p| \ll m_h$ as the heavy mass is taken to infinity. In this case, the correlators can be computed using the original theory but omitting the heavy degrees of freedom, while the corrections to the correlators due to the heavy masses are suppressed by inverse powers of the heavy mass and are of order $\mathcal{O}(\frac{m_l}{m_h}, \frac{|p|}{m_h})$, and the m_h dependence is absorbed to the renormalization of the parameters. The finite temperature theory, however, fails to fulfill the conditions of the theorem. The Appelquist-Carazzone theorem applies only to one, or at most finite number of heavy masses, whereas in the case of the Matsubara modes there is an infinite number of such masses. The physical reason for this failure is that finite temperature generates dynamically new light thermal mass scales, which do not decouple from the long distance physics.

Even if the complete dimensional reduction fails in the sense that the corrections would be of order $\mathcal{O}(\frac{|p|}{T})$, it is still possible to construct a local renormalizable field theory for

the static modes. Consider an action

$$S = \int \mathrm{d}^4x\, \mathcal{L}_{4\mathrm{d}}, \tag{2.44}$$

where the Lagrangian contains only local operators. The action can be split to a part which depends only on the static modes and to a part that contains all the dependence on the non-static modes

$$S(\phi) = S_0(\phi_0(\mathbf{x})) + S_n(\phi_0(\mathbf{x}), \phi_n(x)), \tag{2.45}$$

Now, applying this decomposition, one can formally integrate out the non-static modes giving rise to effective interactions for the static modes

$$\begin{aligned} Z &= \int \mathcal{D}\phi_0 \mathcal{D}\phi_n \exp\left[-S_0(\phi_0(\mathbf{x})) - S_n(\phi_0(\mathbf{x}), \phi_n(x))\right] \\ &= \int \mathcal{D}\phi_0 \exp\left[-S_0(\phi_0(\mathbf{x})) - S_{\mathrm{eff}}(\phi_0(\mathbf{x}))\right], \end{aligned} \tag{2.46}$$

where the quantum fluctuations of the non-static modes are described by an effective interaction

$$\exp(-S_{\mathrm{eff}}(\phi_0(\mathbf{x}))) = \int \mathcal{D}\phi_n \exp(-S_n(\phi_0(\mathbf{x}))). \tag{2.47}$$

If the action of the original theory was renormalizable, the corresponding completely reduced action $S_0(\phi_0(\mathbf{x}))$ is superrenormalizable, as the integral over the Euclidean time gives an overall factor of $1/T$ to the action. This factor is then absorbed to the normalization of the field so that the kinetic term has the canonic unit coefficient rendering the coupling constants dimensionful. On the other hand, the effective interactions arising from the integration out of the non-static modes are neither renormalizable nor local in general. However, the non-static modes have an intrinsic infra-red cutoff proportional to the temperature, and thus they are truly non-local only at length scales comparable and smaller than $1/T$.

At distances much larger than $1/T$, the effective interaction can be expanded as

$$S_{\mathrm{eff}} = \int \mathrm{d}^3x\, \mathcal{L}_{\mathrm{eff}}(\phi_0(\mathbf{x})) \approx \int \mathrm{d}^3x \sum_i g_i(T) Q_i(\phi_0(\mathbf{x})), \tag{2.48}$$

where one writes the non-local terms as an infinite sum of all possible local operators Q_i constructed from the static modes and spatial derivatives with corresponding temperature dependent couplings $g_i(T)$. The low-energy effective theory must have the same symmetries as the original one, so if the effective interaction Lagrangian $\mathcal{L}_{\mathrm{eff}}$ possessed some symmetries inherited from the 4d theory, these propagate to the decomposition and the coefficients of operators breaking these symmetries vanish identically.

The infinite series in Eq. (2.48) can be truncated in a controlled manner, giving an expansion in the scale difference between T and the low energy scale. The only dimensionful quantity in the integral over the non-static modes in Eq. (2.47) is T, and thus the dimensionful couplings g_i originating from the non-static modes have to scale accordingly. The fact that the action is a dimensionless quantity tells us that the dimensional form of the coupling g_i is

$$g_i = \frac{c_i}{T^{\gamma_i - 3}}, \tag{2.49}$$

with a dimensionless coupling c_i and γ_i being the mass dimension of the operator Q_i. The contribution of operator Q_i on a dimensionless observable at low energy scale characterized by E will then be at most $\sim \left(\frac{E}{T}\right)^{\gamma_i - 3}$. Thus, a pronounced scale difference between the low energy physics and the hard scale T allows to truncate the series introducing only small corrections.

To leading order at high temperature, we include only the superrenormalizable operators, and by including systematically operators of higher dimension [42], we can improve our effective theory in powers of E/T. Note that the renormalizable operators of the static action become superrenormalizable operators in the 3d theory and are included in the dimensionally reduced theory. Even if the original theory had contained non-renormalizable operators, they become negligible compared to the superrenormalizable ones when the scale difference is large enough. Thus, the dimensionally reduced effective theory is defined by

$$Z = \int \mathcal{D}\phi_0 \exp\left(\int \mathrm{d}^3x \, \mathcal{L}_{\mathrm{3d}}(\phi_0(\mathbf{x}))\right), \tag{2.50}$$

with the three-dimensional Lagrangian including all the possible superrenormalizable operators that can be constructed from the static fields, respecting the symmetries of the original theory.

The effective theory is of course not predictive until the coefficients g_i of the superrenormalizable operators have been determined. The coefficients have to be determined such that the effective theory reproduces the long distance physics of the original theory, and the way to do this is to match the Green's functions in the two theories. Traditionally, this matching has been carried out within the framework of the weak coupling expansion [9]. However, dimensional reduction is not dependent on weak coupling and it relies only in the scale separation between the temperature and the low energy physics, and thus there is no reason why the matching could not be carried out also non-perturbatively. Some first steps towards this direction have been take in Refs. [3, 43].

The three-dimensional effective theories have three major advantages from the numerical point of view compared to the original one in their regime of validity. First, the theories generated by the dimensional reduction procedure are superrenormalizable, enabling matching between lattice and continuum theory exactly to the desired order of the lattice spacing a in the framework of lattice perturbation theory. Second, the fact that the fermions are integrated out brings a major simplification to the lattice simulations, as there is no need for dynamical fermions, a major nuisance in full theory simulations.

Third, in lattice simulations the physical dimensions of the lattice should be such that the lattice spacing is much smaller than the shortest relevant length scale in the system and at the same time the extent of the lattice should be large enough so that it can accommodate even the longest wavelengths of the physical situation. Thus, if the physical system at study has vast scale differences, one is forced to use huge lattices to meet these conditions. In dimensional reduction, one integrates over the shortest length scale, and thus one can use much larger lattice spacing, leading also to larger volumes.

The superrenormalizability brings along additional challenges as well. In superrenormalizable theories, some parameters of the Lagrangian and local condensates acquire additive cutoff dependence which can be linear or worse. This makes the exact matching inevitable, leading to complex calculations in lattice perturbation theory. Also, in lattice simulations, the signal in the measurements of local operators is dominated by ultra-violet

contributions, exceeding the physical part of the signal by many orders of magnitude. The subtraction of these ultra-violet terms leads to a major significance loss.

Chapter 3

Perturbative dimensional reduction

In this Chapter, Electrostatic QCD (EQCD) and Magnetostatic QCD (MQCD) are discussed. The first of these, electrostatic QCD, describes the static properties of QCD at length scales $\gg T^{-1}$ and the latter at scales $\gg (gT)^{-1}$.

These theories have proven to be very useful in the evaluation of the equation of state, or the pressure, in the weak coupling regime of QCD. It is known how to calculate the weak coupling expansion of the pressure analytically only up to and including the g^5 term. The coefficient of the $g^6 \ln g$ term has also been computed in Ref. [17]; it does not, however, give the next unambiguous contribution to the series until the coefficient of g^6 is determined. In order to improve the result, one would like to extend the calculation to the next order. However, in this case, a sum over infinite numbers of diagrams with arbitrary numbers of loops and with non-trivial topologies [20] would have to be performed. Thus, the g^6 term in the weak coupling expansion may truly be called non-perturbative. This behavior is due to low momentum gluons, which even at high temperature interact strongly. However, in the effective field theory framework, the different theories can be matched via perturbation theory to any desired order free from any infrared problems, so that the problematic infrared regime can be handled within simpler three-dimensional theories. It turns out that using this reduction, the only non-perturbative contribution to order g^6 in pressure is the gluon condensate $\langle \mathrm{Tr}\, F_{ij}^2 \rangle$ of MQCD, which then has to be determined using lattice simulations. For $N_\mathrm{c} = 3$ this has been done in Ref. [44], and the result was generalized to any N_c in Ref. [1].

3.1 Electrostatic QCD

The first three-dimensional effective theory of high temperature QCD we are going to study is Electrostatic QCD, or EQCD, originally proposed in Ref. [10]. The perturbative evaluation of thermodynamical quantities in QCD suffers from severe infrared problems due to the collective excitations in the plasma. Formally, these show up in the perturbative calculations as infra-red divergences which have to be cured by performing resummations of diagrams to all orders in the gauge coupling g, leading to a non-analytic behavior in g. One can, however, perform the resummations elegantly using the effective field theory, and the motivation in using EQCD in Ref. [9] was in fact to simplify such calculations. The effective theory formulation clearly resolves the contributions coming from the different

momentum scales $2\pi T$, gT, and g^2T. We use the term EQCD to denote the theory generalized to any SU(N_c) gauge group.

The action of EQCD is obtained by performing Fourier decomposition along the Euclidean time direction to the fields in Eq. (2.13), and applying the dimensional reduction procedure outlined in the previous Chapter. The remaining degrees of freedom are the static modes of magnetic gauge fields A_i and of the color-electric gauge field A_0:

$$S_{\rm EQCD} = \int \mathrm{d}^d x\, \mathcal{L}_{\rm EQCD} \tag{3.1}$$

$$\begin{aligned}\mathcal{L}_{\rm EQCD} &= -p_{\rm E} + \frac{1}{2}\mathrm{Tr}\, F_{ij}F_{ij} + \mathrm{Tr}\,(D_iA_0)^2 + (m_{\rm E}^{\rm bare})^2\,\mathrm{Tr}\, A_0^2 \\ &\quad +\lambda_{\rm E}^{(1)}\mathrm{Tr}\,(A_0^2)^2 + \lambda_{\rm E}^{(2)}\mathrm{Tr}\, A_0^4,\end{aligned} \tag{3.2}$$

with $d = 3 - 2\epsilon$. The action consists of all superrenormalizable gauge invariant operators respecting local gauge symmetry and the discrete C, P, and T symmetries. The renormalizable and non-renormalizable terms have been omitted since these operators do not contribute at order $\mathcal{O}(g^6)$ to the equation of state.

The color-electric field transforms in the adjoint representation under static gauge transformations as

$$A_0(\mathbf{x}) \to \Omega(\mathbf{x})A_0(\mathbf{x})\Omega^{-1}(\mathbf{x}). \tag{3.3}$$

The covariant derivative $D_i = \partial_i + ig_{\rm E}[A_i, \cdot\,]$ is also in the adjoint representation and the indices $i, j = 1 \ldots d$ go only over the spatial directions. Here, the field strength tensor is given by

$$F_{ij} = \partial_i A_j - \partial_j A_i + ig_{\rm E}[A_i, A_j]. \tag{3.4}$$

The cubic term $\mathrm{Tr}\, A_0^3$ and the quintic terms $\mathrm{Tr}\, A_0^2\mathrm{Tr}\, A_0^3$ and $\mathrm{Tr}\, A_0^5$ are absent in the Lagrangian of Eq. (3.1) due to the discrete symmetries of the full theory Lagrangian [19]. The transformation properties of the fields in the dimensionally reduced theory under the discrete symmetries of the full theory C, P, and T, are shown in Table 3.1. Note that introducing a chemical potential for fermions breaks the discrete symmetries and makes the coefficient of the cubic operator non-zero [14]. However, even though there is no symmetry restricting the quintic terms in the finite chemical potential, the coefficients have been found to be equal to zero at 1-loop and 2-loop levels [14, 45]. In the case of SU(2), the cubic term is in fact always identically zero as the symmetric structure constants of the group vanish.

We regulate the theory in the $\overline{\rm MS}$ scheme, with the renormalization scale being $\bar{\mu}_{\rm E} = \mu_{\rm E}\,(e^{\gamma}/4\pi)^{-1/2}$. Note that the renormalization scale of the three-dimensional theory $\mu_{\rm E}$ is independent of the renormalization scale of the four-dimensional theory, and it is usually chosen to be $g_{\rm E}^2$. From now on we always implicitly assume that the factor $\mu^{-2\epsilon}$ is attached to the coupling constants, so that the dimensionalities of the coupling constants $(g_E^2, \lambda_{\rm E}^{(1)}, \lambda_{\rm E}^{(2)})$ are always GeV. As the Lagrangian is superrenormalizable, there is only a finite number of diagrams contributing to its renormalization and the dependence of the $\overline{\rm MS}$ renormalization scale $\bar{\mu}_{\rm E}$ can be solved exactly. All the parameters of the action are

	C	P	T	Z(N_c)
A_0	A_0^*	A_0	$-A_0$	$A_0 + 2\pi nT/(g_E N_c)$
A_i	$-A_i^*$	$-A_i$	$-A_i$	A_i

Table 3.1: The transformation of the degrees of freedom in the dimensionally reduced theory under the discrete symmetries of the full theory C, P and T. The fields are in Euclidean space and the transformation properties of A_0 under T differs from that in Minkowski space [19]. The action in Eq. (3.1) is invariant in C, P and T but is not invariant under Z(N_c).

scale invariant, except the mass term, which is additively renormalized by [46, 47]

$$(m_E^{\rm bare})^2 = m_E^2(\bar{\mu}_E) + \frac{1}{(4\pi)^2} f_2 \frac{\mu_E^{-4\epsilon}}{4\epsilon} \tag{3.5}$$

$$\begin{aligned} f_2 = {} & 2N_c g_E^2 \left[\left({N_c}^2+1\right)\lambda_E^{(1)} + \left(2{N_c}^2-3\right)\frac{\lambda_E^{(2)}}{N_c} \right] - 2\left({N_c}^2+1\right)\lambda_E^2 \\ & -4\left(2{N_c}^2-3\right)\lambda_E^{(1)}\frac{\lambda_E^{(2)}}{N_c} - \left({N_c}^4-6{N_c}^2+18\right)\left(\frac{\lambda_E^{(2)}}{N_c}\right)^2 . \end{aligned} \tag{3.6}$$

This exact counterterm is sufficient to keep all the n-point Green's functions in the effective theory, with $n > 0$, finite.

Compared to the complete dimensional reduction, the interactions with the non-static modes have generated three new terms in the Lagrangian, a mass term m_E for the color-electric field, and two four-point interactions $\lambda_E^{(1)}$ and $\lambda_E^{(2)}$. In the case of SU(2) and SU(3), there is a special relation between the two traces

$$\mathrm{Tr}\, A_0^4 = \frac{1}{2}(\mathrm{Tr}\, A_0^2)^2, \qquad N_c = 2, 3 \tag{3.7}$$

so that in the case of these groups, there is only one independent four-point coupling $\lambda_E \equiv \lambda_E^{(1)} + \frac{1}{2}\lambda_E^{(2)}$. Thus, for $N_c = 2, 3$, the dynamics of the theory is governed by the two dimensionless (in $\epsilon \to 0$ limit) ratios

$$x \equiv \lambda_E / g_E^2 \tag{3.8}$$

$$y \equiv m_E^2(g_E^2)/g_E^4 \tag{3.9}$$

and an overall mass scale g_E^2. In addition to these, there is the unit operator p_E , which governs the contributions to the partition function arising from the non-static modes.

In the very high temperature regime where the coupling constant g is small, the coefficients can be matched to the full theory using perturbation theory, in principle up to any desired order in the renormalized coupling $g^2(\bar{\mu}_{4d})$. In particular, the mass term has the expansion

$$m_E^2(\bar{\mu}_E) \sim g^2(\bar{\mu}_{4d})T^2 + \mathcal{O}(g^4) \tag{3.10}$$

and it is easy to see that the dynamically generated mass coming from the collective effect of the non-static modes becomes light compared to the temperature in the weak coupling

limit. This provides the scale difference between the hard scale $\sim T$ and low energy scale $\sim m_{\rm E}$, required to truncate expansion in Eq.(2.48); the effect of higher order operators to the dimensionless observables is suppressed by high powers of $m_{\rm E}/T \sim g$.

The pressure (or minus the free energy density) of the 4d theory can be written using the action of EQCD in the form

$$p_{\rm QCD}(T) \;=\; \lim_{V\to\infty}\frac{T}{V}\ln\int \mathcal{D}A_k\mathcal{D}A_0\exp(-S_{\rm EQCD}), \tag{3.11}$$

where V denotes the d-dimensional volume. In order to compute the pressure up to order g^6, the parameters have to be matched to a sufficient depth, namely [17]

$$\begin{aligned}
\mu_{\rm E}^{2\epsilon}p_{\rm E}(T) &= T^4\Big[\alpha_{\rm E1}+g^2\Big(\alpha_{\rm E2}+\mathcal{O}(\epsilon)\Big) \\
&\quad +\frac{g^4}{(4\pi)^2}\Big(\alpha_{\rm E3}+\mathcal{O}(\epsilon)\Big)+\frac{g^6}{(4\pi)^4}\Big(\beta_{\rm E1}+\mathcal{O}(\epsilon)\Big)+\mathcal{O}(g^8)\Big], &(3.12)\\
m_{\rm E}^2(g_{\rm E}^2) &= T^2\Big[g^2\Big(\alpha_{\rm E4}+\alpha_{\rm E5}\epsilon+\mathcal{O}(\epsilon^2)\Big) &(3.13)\\
&\quad +\frac{g^4}{(4\pi)^2}\Big(\alpha_{\rm E6}+\beta_{\rm E2}\epsilon+\mathcal{O}(\epsilon^2)\Big)+\mathcal{O}(g^6)\Big], &(3.14)\\
\mu_{\rm E}^{-2\epsilon}g_{\rm E}^2 &= T\Big[g^2+\frac{g^4}{(4\pi)^2}\Big(\alpha_{\rm E7}+\beta_{\rm E3}\epsilon+\mathcal{O}(\epsilon^2)\Big)+\mathcal{O}(g^6)\Big], &(3.15)\\
\mu_{\rm E}^{-2\epsilon}\lambda_{\rm E}^{(1)} &= T\Big[\frac{g^4}{(4\pi)^2}\Big(\beta_{\rm E4}+\mathcal{O}(\epsilon)\Big)+\mathcal{O}(g^6)\Big], &(3.16)\\
\mu_{\rm E}^{-2\epsilon}\lambda_{\rm E}^{(2)} &= T\Big[\frac{g^4}{(4\pi)^2}\Big(\beta_{\rm E5}+\mathcal{O}(\epsilon)\Big)+\mathcal{O}(g^6)\Big]\,, &(3.17)
\end{aligned}$$

where $g=g(\bar\mu_{\rm 4d})$. Here, the coefficients $\alpha_{\rm E}$ and $\beta_{\rm E}$ have been explicitly named such that only the $\alpha_{\rm E}$ are needed at order $\mathcal{O}(g^6\ln(g))$, while at the full order $\mathcal{O}(g^6)$ also the $\beta_{\rm E}$ are needed. The actual numerical values of all $\alpha_{\rm E}$ are known and given in Ref. [17]. Some of the $\beta_{\rm E}$ are also known [11, **?**, 48] but the matching coefficient $\beta_{\rm E1}$ remains undetermined, and its computation requires the evaluation of all the four-loop vacuum diagrams of the full theory without resummations. The first steps towards this computation can be found in Ref. [49]. As for now, this is the only unknown part (for $N_{\rm c}=3$) of the $\mathcal{O}(g^6)$ pressure, as the functional integral in Eq. (3.11) can be evaluated to order g^6 by doing a further simplification to the theory, i.e., mapping EQCD to three-dimensional pure Yang-Mills theory.

The matching conditions in Eqs. (3.12)-(3.17) define a subspace in the parameter space of EQCD, where the theory describes QCD. On the (x,y)-plane (for $N_{\rm c}=2,3$), we find that in the weak coupling limit, there is relation between the two parameters

$$xy \;=\; \frac{\alpha_{\rm E1}\left(\beta_{\rm E4}-\frac{1}{2}\beta_{\rm E5}\right)}{4\pi^2}+\mathcal{O}(x)=\frac{(N_{\rm c}+\frac{1}{2}N_{\rm f})(N_{\rm c}-N_{\rm f}+6)}{72\pi^2}+\mathcal{O}(x), \tag{3.18}$$

which is called the 4d-matching line.

3.2 Phase structure of EQCD

The phase diagram of EQCD has been studied in [12, 13, 50, 51, 52]. The studies have restricted to $N_{\rm c}=2$, 3 and 5. For $N_{\rm c}=2$ the phase diagram has been measured using

lattice simulations, and supplemented with a two-loop calculation of the effective potential. The results are reproduced in Fig. 3.1. The phase diagram does not correspond to the physical phase diagram of QCD; there is no deconfinement transition present in EQCD. However, there are some features which in a non-trivial way resemble those of the full theory.

For SU(2), there are no additional global symmetries present in the action of EQCD in Eq. (3.1). Note that the transformation

$$A_0 \to -A_0 \tag{3.19}$$

is part of the local gauge group and thus cannot be broken spontaneously. Nevertheless, there is a phase transition in the theory, where the expectation values of various operators such as $\langle \mathrm{Tr}\, A_0^2 \rangle$ and $\langle (\mathrm{Tr}\, A_0^2)^2 \rangle$ change in a singular fashion as functions of x and y: Given a fixed x, the expectation values of these operators are large when $y < y_c$, and small when $y > y_c$. In the limit where $x \to 0$, the phase transition becomes infinitely strong (characterized by the interface tension), allowing the use of a semi-classical approximation, and the intersection point and the slope of the critical curve at $x \to 0$ can be analytically evaluated

$$y_c(x) = \frac{2}{9\pi^2 x} + \frac{1}{4\pi^2} + \mathcal{O}(x). \tag{3.20}$$

The strong first order transition is associated with a sizable region of metastability. At larger x, the semi-classical approximation fails and lattice simulations become necessary. The simulations show that the first order transition line has a second order endpoint at $x \sim 0.3$, while at larger values of x, the transition is merely a cross-over.

In the case of SU(3), the transformation in Eq. (3.19) is a global symmetry of the theory and is distinct from the local gauge group. There is also a genuine order parameter $\langle \mathrm{Tr}\, A_0^3 \rangle$, associated with the symmetry. The order parameter is identically zero in the symmetric phase $y > y_c$ and obtains a non-zero vacuum expectation value in the broken phases $y < y_c$, signalling the spontaneous breaking of the symmetry. Due to the order parameter, there are actually two distinct equivalent broken phases with $\langle \mathrm{Tr}\, A_0^3 \rangle = \pm |\langle \mathrm{Tr}\, A_0^3 \rangle|$, in addition to the symmetric phase. Again, at small x, there is a first order transition separating the symmetric phase and the broken phases. At $x \to 0$ the transition lies at

$$y_c(x) = \frac{3}{8\pi^2 x} + \frac{9}{16\pi^2} + \mathcal{O}(x). \tag{3.21}$$

At larger x, the first order transition line terminates at a tricritical point at $x \sim 0.25$, and beyond the tricritical point, the transition becomes a second order one.

There is a striking remnant of the $\mathrm{Z}(N_\mathrm{c})$ symmetry in the phase diagram of EQCD. In the absence of dynamical quarks, the case where the center symmetry of QCD is exact, the 4d-matching line in Eq. (3.18) coincides with the first order phase transition lines in Eqs. (3.20) and (3.21), such that in the case of $N_\mathrm{c} = 2$ there are two, and for $N_\mathrm{c} = 3$ three coexisting phases. This gives a natural interpretation to the (strictly speaking unphysical) broken phases in EQCD: The broken phases correspond to the other $\mathrm{Z}(N_\mathrm{c})$ vacua, for which $\langle L \rangle \neq 1$. However, the matching is not exact and the physics in the broken phases is not equivalent with the symmetric one: Various condensates and screening masses measured in the broken phase differ largely from those measured in the symmetric phase. Still, it is remarkable that EQCD, which has been constructed applying perturbation theory around

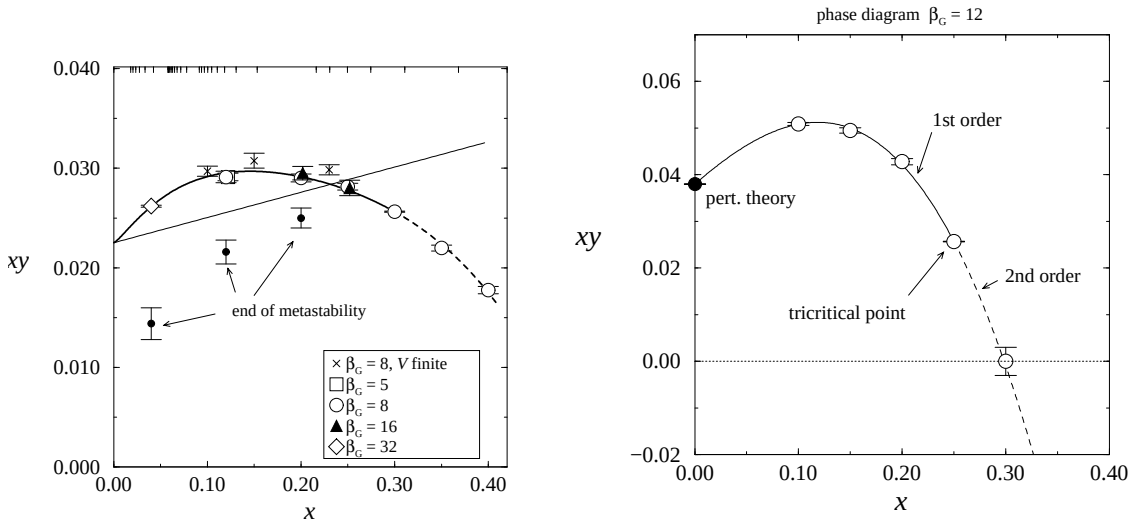

Figure 3.1: The phase diagrams of EQCD in the thermodynamical limit with $N_{\rm c} = 2$ (left)[12] and $N_{\rm c} = 3$ (right)[13]. The symmetric phase is at large and the broken at small xy. At small $x = \lambda_{\rm E}/g_{\rm E}^2$ there is a first order transition for both $N_{\rm c}$. The points at $x \to 0$ are calculated in perturbation theory and coincide with the 4d→3d perturbative matching curve (straight line in the left panel). For $N_{\rm c} = 2$, the first order line terminates to a second order critical point and continues as a cross-over. For $N_{\rm c} = 3$ the first order line terminates to a tricritical point and for larger values of x the transition is of second order.

the $\langle L \rangle = 1$ vacuum, dynamically generates a phase structure that emulates that of full QCD in this non-trivial way.

One is tempted to consider the possibility that the true all-orders 4d-matching line would follow the transition line of the 3d theory. Then it could be plausible to identify the end point of the first order transition with the physical deconfinement transition in the full QCD. This picture is not, however, correct as the inclusion of the higher order contributions deflects the 4d-matching line from the critical curve: The expansion of the critical curve is in powers of $x^{1/2}$, while the matching generates only terms that are integer powers of x. This can be cured only by including non-renormalizable operators in the action.

It is noteworthy that at small but non-zero x, the perturbative 4d-matching line actually lies in the part of the phase diagram where the symmetric physical minimum is metastable. From a practical point of view this does not, however, pose a problem: At small x, the metastability allows one to perform simulations in the symmetric phase. The associated interface tension scales as $\sim x^{-5/3}$, preventing tunneling into the global minima in any realistic simulations.

The inclusion of light dynamical quarks modifies the 4d-matching curve such that it no longer coincides with the phase transition line. This comes as no surprise because the quarks break the $\mathrm{Z}(N_{\rm c})$ symmetry and there is no reason to expect coexisting phases in the three-dimensional theory either.

3.3 Magnetostatic QCD

At very high temperature, in the physical symmetric phase, the long distance properties of EQCD can be described using an even simpler effective field theory. In addition to the mass of the color-electric field $m_{\rm E} \sim gT$, EQCD has another scale in it, namely the scale arising from the color-magnetic sector. Parametrically this scale is of order $g_{\rm E}^2 = g^2 T$, and in the weak coupling limit the color-electric scale becomes heavy compared to it. This separation of scales, however, gets realized only at extremely high temperatures; simulations show that this picture is valid only at temperatures $T \gg 100 T_c$ [14]. In fact, at temperatures below $100 T_c$, the non-perturbative features of the theory render the color-electric mass lighter than the lightest color-magnetic glue-ball, in contrast to the naive perturbative expectations. Nevertheless, above this temperature, it is possible to push the effective theory approach even further by analytically integrating out the heavy scale gT in perturbation theory. In this case, the resulting action will be simply (in $\overline{\rm MS}$-renormalization scheme)

$$S_{\rm MQCD} = \int {\rm d}^d x \, \mathcal{L}_{\rm MQCD} \tag{3.22}$$

$$\mathcal{L}_{\rm MQCD} = \frac{1}{2} {\rm Tr}\, F_{ij} F_{ij} - p_{\rm E} - p_{\rm M}, \tag{3.23}$$

with $d = 3 - 2\epsilon$. The field strength tensor reads again

$$F_{ij} = \partial_i A_j - \partial_j A_i + i g_{\rm M} [A_i, A_j], \tag{3.24}$$

where the only difference from the corresponding quantity in EQCD is the coupling constant g_M, which is to be matched so that the long distance Green's functions of the static color-magnetic fields match between the two theories. The coefficient $p_{\rm M}$ contains the contribution of the color-electric modes to the pressure. To compute the pressure up to g^6, the parameters are matched to

$$\begin{aligned}
\frac{p_{\rm M}(T)}{T \mu^{-2\epsilon}} &= \frac{1}{(4\pi)} d_A m_{\rm E}^3 \left[\frac{1}{3} + \mathcal{O}(\epsilon) \right] \\
&+ \frac{1}{(4\pi)^2} d_A N_{\rm c} g_{\rm E}^2 m_{\rm E}^2 \left[-\frac{1}{4\epsilon} - \frac{3}{4} - \ln \frac{\bar{\mu}}{2 m_{\rm E}} + \mathcal{O}(\epsilon) \right] \\
&+ \frac{1}{(4\pi)^3} d_A {N_{\rm c}}^2 g_{\rm E}^4 m_{\rm E} \left[-\frac{89}{24} - \frac{1}{6}\pi^2 + \frac{11}{6} \ln 2 + \mathcal{O}(\epsilon) \right] \\
&+ \frac{1}{(4\pi)^4} d_A {N_{\rm c}}^3 g_{\rm E}^6 \left[\alpha_{\rm M} \Big(\frac{1}{\epsilon} + 8 \ln \frac{\bar{\mu}}{2 m_{\rm E}} \Big) + \beta_{\rm M} + \mathcal{O}(\epsilon) \right] \\
&+ \frac{1}{(4\pi)^2} d_A (d_A + 2) \lambda_{\rm E}^{(1)} m_{\rm E}^2 \left[-\frac{1}{4} + \mathcal{O}(\epsilon) \right] \\
&+ \frac{1}{(4\pi)^2} d_A \frac{2 d_A - 1}{N_c} \lambda_{\rm E}^{(2)} m_{\rm E}^2 \left[-\frac{1}{4} + \mathcal{O}(\epsilon) \right], \qquad (3.25) \\
g_{\rm M}^2 &= g_{\rm E}^2 \left(1 + \mathcal{O}(g_{\rm E}^2 / m_{\rm E}) \right), \qquad (3.26)
\end{aligned}$$

with $d_A = {N_{\rm c}}^2 - 1$. In the action, the only fields present are the static magnetic gluons A_i. Also, there is only one dimensionful scale, the gauge coupling $g_{\rm M}$.

The pressure of full QCD can again be written up to and including order g^6 using the MQCD action

$$p_{\rm QCD}(T) = \lim_{V\to\infty}\frac{T}{V}\ln\int\mathcal{D}A_i\exp(-S_{\rm MQCD}), \tag{3.27}$$

$$\equiv p_{\rm E}+p_{\rm M}+p_{\rm G}, \tag{3.28}$$

where we have defined the pressure of three-dimensional Yang-Mills theory

$$p_{\rm G} = \lim_{V\to\infty}\int\mathcal{D}A_i\exp(-S_{\rm YM}), \tag{3.29}$$

with

$$S_{\rm YM} = \int {\rm d}^3x\mathcal{L}_{\rm YM} \tag{3.30}$$

$$\mathcal{L}_{\rm YM} = \frac{1}{2}{\rm Tr}\,F_{ij}F_{ij}. \tag{3.31}$$

The pure gauge theory is an inherently non-perturbative theory. A simple way to see this is to consider any Feynman diagram that can be constructed in the theory. Since there are no mass scales present in the pure gauge propagator (in covariant gauge fixing)

$$G_{ij}(\mathbf{k}) = \frac{1}{\mathbf{k}^2}\left(\delta_{ij}-(1-\xi)\frac{\mathbf{k}_i\mathbf{k}_j}{\mathbf{k}^2}\right), \tag{3.32}$$

ultra-violet divergences in any diagram cancel exactly against the infrared divergences [47], leading to the vanishing of the diagram.

The $\overline{\rm MS}$-scale dependence along with the coefficient of the $\mathcal{O}(g^6\ln g)$ term can, however, be computed in perturbation theory by evaluating the ultraviolet divergence in $p_{\rm G}$ by separating the infrared regime from the ultraviolet. In practice, one performs the separation by including a gluon mass term in the Lagrangian. After identifying the logarithm,the mass can be sent to zero.

$$\mu_{\rm M}^{2\epsilon}p_{\rm G} = T({N_{\rm c}}^2-1){N_{\rm c}}^3\frac{g_{\rm M}^6}{(4\pi)^4}\left[\alpha_{\rm G}\left(\frac{1}{\epsilon}+8\ln\frac{\bar{\mu}_{\rm M}}{2N_{\rm c}g_{\rm M}^2}\right)+B_{\rm G}\right], \tag{3.33}$$

where $\bar{\mu}_{\rm M}$ is the $\overline{\rm MS}$-renormalization scale of MQCD and does not in principle have to be the same as $\bar{\mu}_{\rm E}$. The coefficient $\alpha_{\rm G}$ has been computed in Ref. [47] and has the value

$$\alpha_{\rm G} = \frac{43}{96}-\frac{157}{6144}\pi^2 \approx 0.195715. \tag{3.34}$$

What is left to be determined, is the infrared sensitive part of the pressure $B_{\rm G}$. Here, perturbation theory cannot help any more and the theory has to be formulated on a discrete lattice.

Using standard Wilson discretization, the corresponding action on the lattice reads

$$S_{\rm YM}^a = \beta\sum_{\mathbf{x}}\sum_{k<l}^{3}\left(1-\frac{1}{N_{\rm c}}{\rm ReTr}\,[P_{kl}(\mathbf{x})]\right), \tag{3.35}$$

where P_{kl} is the plaquette given in Eq. (2.24). In three dimensions the lattice coupling β is related to the lattice spacing by

$$\beta \equiv \frac{2N_{\rm c}}{a g_{\rm M}^2}, \tag{3.36}$$

and the continuum limit is reached linearly as $\beta \to \infty$.

Analogously to $\overline{\rm MS}$, the pressure of MQCD can be defined on the lattice

$$p_{\rm G}^a = \lim_{V\to\infty} \frac{T}{V} \ln \left[\int \mathcal{D}U_k \exp(-S_{\rm YM}^a) \right], \tag{3.37}$$

which obtains the same contributions from the long-wavelength modes as its continuum counterpart $p_{\rm G}$. However, the ultraviolet sectors of the two regularizations are very different and the effects of the finite lattice spacing need to be removed by renormalizing the pressure. Again, as the theory is superrenormalizable, there are only a finite number of additive counterterms needed (to a given order in a), all calculable within lattice perturbation theory. For dimensional reasons, the lattice spacing dependence has to come from terms of the form $g_{\rm M}^{2n} a^{n-3}$ (with logarithms). Choosing $\mu_{\rm M} = g_{\rm M}^2$, the continuum $\overline{\rm MS}$ pressure can finally be written

$$\begin{aligned} \frac{p_{\rm M}}{T} &= \frac{p_{\rm M}^a}{T} + C_1 \frac{1}{a^3} \left(\ln \frac{1}{a g_{\rm M}^2} + C_1' \right) + C_2 \frac{g_{\rm M}^2}{a^2} \\ &\quad + C_3 \frac{g_{\rm M}^4}{a} + C_4 g_{\rm M}^6 \left(\ln \frac{1}{a g_{\rm M}^2} + C_4' \right) + \mathcal{O}(g_{\rm M}^8 a), \end{aligned} \tag{3.38}$$

which becomes exact in the continuum limit.

By taking derivatives of Eq. (3.38) with respect to $g_{\rm M}$ and using 3d rotational and translational symmetries, the infrared sensitive contribution to the pressure can be written as

$$8 \frac{d_A {N_{\rm c}}^6}{(4\pi)^4} B_{\rm G}(N_{\rm c}) = \lim_{\beta\to\infty} \beta^4 \left\{ \langle 1 - \frac{1}{N_{\rm c}} {\rm Tr}\, [P] \rangle_a - \left[\frac{c_1}{\beta} + \frac{c_2}{\beta^2} + \frac{c_3}{\beta^3} + \frac{c_4}{\beta^4} (\ln\beta + c_4') \right] \right\}, \tag{3.39}$$

where the argument of $B_{\rm G}$ is explicitly written to remind us that it is a function of $N_{\rm c}$ only. The numerical values of the coefficients $c_1 \ldots c_4$ are known from Refs. [53, 54] and read

$$c_1 = \frac{{N_{\rm c}}^2 - 1}{3}, \tag{3.40}$$

$$c_2 = d_A {N_{\rm c}}^2 \left(0.03327444(8) - \frac{1}{18} \frac{1}{{N_{\rm c}}^2} \right), \tag{3.41}$$

$$c_3 = d_A {N_{\rm c}}^4 \left(0.0147397(3) - 0.04289464(7) \frac{1}{{N_{\rm c}}^2} + 0.04978944(1) \frac{1}{{N_{\rm c}}^4} \right), \tag{3.42}$$

$$c_4 = 0.000502301323 d_A {N_{\rm c}}^6, \tag{3.43}$$

with $d_A = {N_{\rm c}}^2 - 1$. The numerical value of the coefficient c_4', describing the constant difference between the two schemes is, however, known only for $N_{\rm c} = 3$, where it has been evaluated using numerical stochastic lattice perturbation theory [55]:

$$c_4' \Big|_{N_{\rm c}=3} = 7.0(3). \tag{3.44}$$

3.4 Simulation results in MQCD

In this Section, we review some results from numerical simulations performed in order to determine $B_G(N_c)$, the only non-perturbative input needed for the weak coupling expansion of the pressure of high temperature QCD up to and including $\mathcal{O}(g^6)$. The $N_c = 3$ case was completed in Ref. [44] and the work was generalized to arbitrary N_c in Ref. [1], by performing simulations for $N_c = 2, 4, 5$, and 8.

Because the last matching coefficient c_4' is unknown, we defined a substituting quantity through

$$P_{\rm G}(\beta, N_{\rm c}) \equiv \frac{32\pi^4\beta^4}{d_A {N_{\rm c}}^6} \left\{ \langle 1 - \frac{1}{N_{\rm c}} {\rm Tr}\,[P] \rangle_a - \left[\frac{c_1}{\beta} + \frac{c_2}{\beta^2} + \frac{c_3}{\beta^3} + \frac{c_4}{\beta^4} \ln\beta \right] \right\}, \tag{3.45}$$

which is easily related to the original non-perturbative input

$$B_{\rm G}(N_{\rm c}) - \left(\frac{43}{12} - \frac{157}{768}\pi^2 \right) c_4' = P_{\rm G}(\infty, N_{\rm c}). \tag{3.46}$$

The recipe to obtain the function $P_{\rm G}(\infty, N_{\rm c})$ is to measure the plaquette expectation value at different values of β and subtract the ultraviolet divergences. Then, the extrapolations to infinite volume and continuum limit need to be taken, after which the functional form of $P_{\rm G}(\infty, N_{\rm c})$ can be fitted.

It is important to estimate the dimensions of the lattice, so that it can accommodate the physically relevant scales. Here, the only dynamical scale is the correlation length of the lightest glueball, which scales as $1/N_{\rm c}g_{\rm M}^2$ [56, 57]. In order to describe the correct physics, we must thus impose the condition

$$a \ll \frac{1}{N_{\rm c} g_{\rm M}^2} \ll Na. \tag{3.47}$$

When using lattice spacings that fulfill this condition, we observe that the signal is overwhelmed by the ultraviolet contribution by five orders of magnitude, which gives rise to a need to use large statistics and supercomputing to compensate the massive significance loss (Fig. 3.2).

The simulation results for non-perturbative input $P_G(\infty, N_{\rm c})$ are shown in Fig. 3.3. The data is well described by a linear fit

$$P_G(\infty, N_{\rm c}) = 15.9(2)\left(1 - 2.8(1)/{N_{\rm c}}^2\right), \qquad \chi^2/\text{d.o.f.} = 5.4/3. \tag{3.48}$$

The term ${N_{\rm c}}^{-1}$ provides a bad description of the data or is zero within the accuracy. It is not surprising that the input seems to be a function of ${N_{\rm c}}^{-2}$ rather ${N_{\rm c}}^{-1}$. As there is no fundamental matter in the theory, the large $N_{\rm c}$ expansion has only terms proportional to ${N_{\rm c}}^{-2}$ [58].

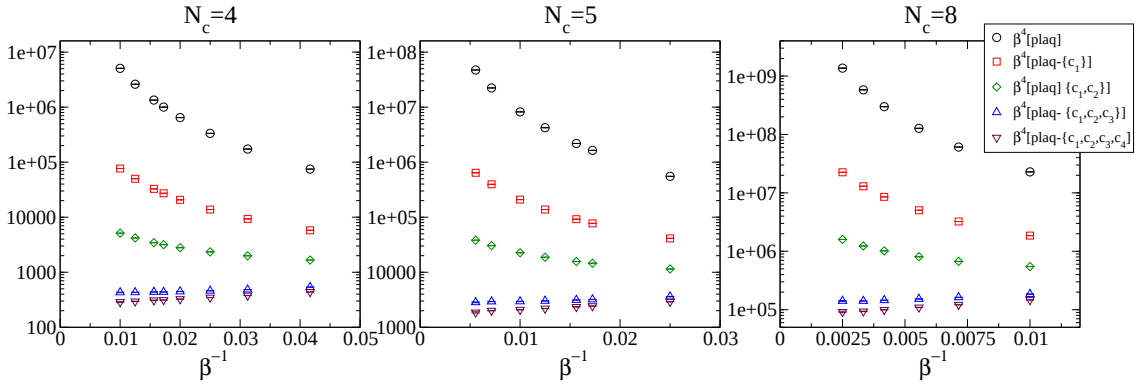

Figure 3.2: The significance loss due to the subtraction of ultraviolet divergences in the plaquette expectation value with different N_c. Here "plaq"$\equiv \langle 1 - \frac{1}{N_c}\mathrm{Tr}\,[P_{ij}]\rangle$ and the symbols c_i in curly brackets indicate which subtractions of Eq. (3.39) have been taken into account.

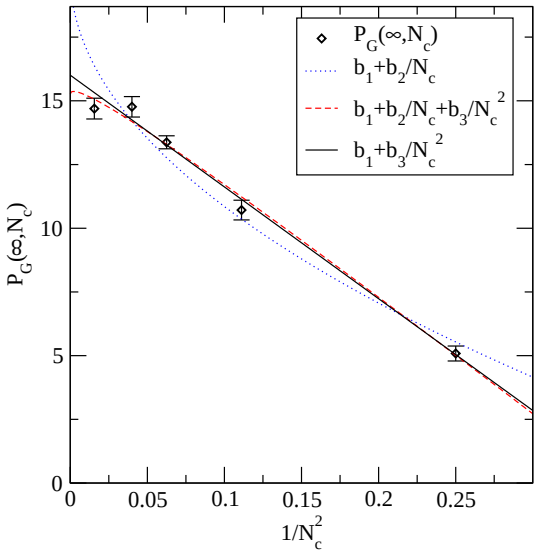

Figure 3.3: Comparing different fits for higher order terms in N_c. The term ${N_c}^{-1}$ is zero within our resolution implying that P_G is a function of ${N_c}^{-2}$.

Chapter 4

Center symmetric effective theories

The dimensionally reduced effective theories introduced in the previous Chapter describe the long distance properties of static correlators of QCD well at high enough temperatures. What is meant by high enough seems to be, depending on the observable, somewhere between $2T_c$ and $10T_c$ [14]. We would like to answer the question: What makes the effective theories fail at lower temperatures, such that they fail to capture the approach towards the deconfinement transition?

There are three independent approximations made in the construction of EQCD:

- The gauge fields were expanded around one of the N_c deconfining vacua explicitly mutilating the $Z(N_c)$-symmetry of the (quarkless) 4d theory, on the basis that the symmetry is spontaneously broken at high T.
- The marginal and non-renormalizable operators were neglected due to a scale difference between the color-electric/color-magnetic sector and the scale set by the temperature.
- The couplings of the effective theory were matched through a weak coupling expansion.

In the case of MQCD, the first condition is clearly not well motivated below $100T_c$ as the electric screening mass becomes lighter than the magnetic one. In the case of EQCD, the situation is not as clear. At $T = 2T_c$, the electric screening mass for the quarkless case is $m_D/T = 2.71(6)$ (see also Fig. 4.1) for SU(3) and is of the same order also for SU(2)[59, 60]. This of course does not look like a suitable expansion parameter, but considering that the mass scale that is associated with the Matsubara modes is actually $2\pi T$, and it may or may not be reasonable to use $m_D/(2\pi T) \sim 0.4$ to truncate the action of the effective theory.

The perturbative matching of the parameters converges relatively fast: At $T = T_c$ the value of the gauge coupling is $g^2/4\pi \sim 0.2$ for SU(3)[11]. While the loop-corrections are certainly significant, the parameters are not obviously non-perturbative either.

Even if the integration out of the hard modes could be performed using the weak coupling expansion, the dynamics of the perturbative setup around one deconfining minimum cannot accommodate the non-trivial vacuum structure close to the phase transition, as the transition is driven by the tunneling of the Polyakov loop between different vacua. At

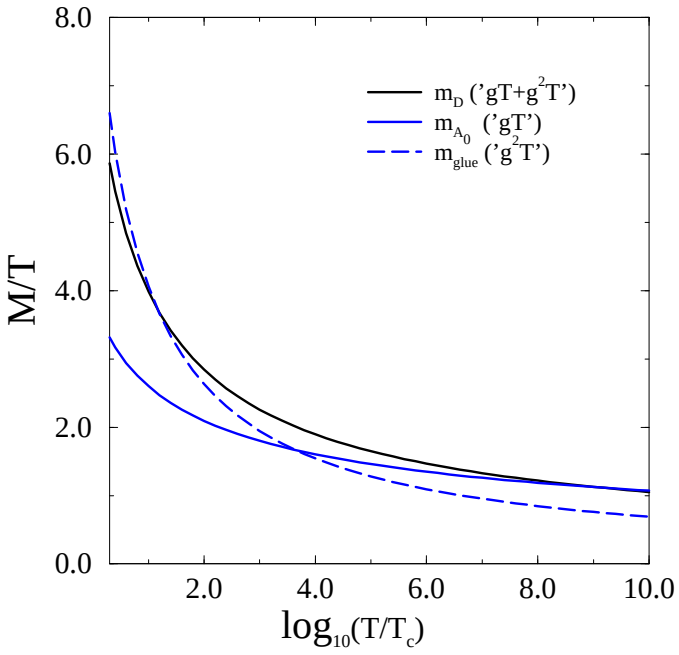

Figure 4.1: The temperature dependence of the two lowest 0_+^{++} and the lowest 0_-^{-+} states in SU(3) pure gauge theory as taken from Refs. [14, 25]. The smallest screening mass is still moderately below the hard scale $2\pi T$ even near T_c. At $T \sim 1000 T_c$, the color-magnetic screening mass (dashed line) becomes heavier than color-electric one (lower solid line) contrary to the naive perturbative intuition, inhibiting the description of the plasma with MQCD.

the $\langle L \rangle \neq 0$ minima, the color-electric field takes values $A_0 \sim \frac{T}{g}$ and clearly a description constructed from order g fluctuations around the trivial vacuum is not justified when the other minima become important for the dynamics of the system.

A natural remedy would be to use the corresponding lattice quantity U_0, to describe the color-electric field. However, the Wilson line is a unitary matrix and an effective theory with polynomial interactions formulated in terms of it would not be a renormalizable one. For an effective theory, this is not a fundamental problem since the ultraviolet cutoff keeps the theory finite, nevertheless it is a major practical nuisance. Such theories are discussed e.g. in Ref. [61].

An alternative solution was introduced in Ref. [23], where an effective theory for *coarse-grained* Wilson loops was constructed for the gauge group SU(3), and the theory was formulated on the lattice in Ref. [2]. The blocking does not conserve the unitarity property of the matrices and a superrenormalizable field theory with polynomial interactions can be constructed. An effective theory for SU(2) coarse-grained Wilson lines both in the continuum and on the lattice was constructed in Ref. [3]. In the following, both theories are introduced in continuum formulation, while the lattice formulation of these theories is discussed in detail in the papers [2, 3] included in this thesis.

The matching of the effective theories to the 4d theory is performed to the leading order of perturbation theory by imposing a condition that the theories reduce to EQCD at high

temperature, and by matching the domain wall profiles between two deconfining minima at the semi-classical level. The first condition ensures that to a given order in perturbation theory, the theories have the predictive power of EQCD, while at the same time, the domain wall matching captures the phase structure of the full theory. This perturbative matching procedure, however, leaves some parameters of the Lagrangian undetermined: For SU(2) there is one undetermined parameter and for SU(3) two. These parameters describe the physics of the effective theory at the scale T, which is left undetermined, as the theory is constructed to be applicable only in the low energy regime.

4.1 Center symmetric effective theory for hot SU(2) Yang-Mills theory

The degree of freedom in the center symmetric effective theories is the coarse-grained Wilson loop. The coarse-graining needs to be performed in a gauge invariant manner, and this is achieved by parallel transporting all the Wilson lines inside a block to a single point representing the block

$$\mathcal{Z}(\mathbf{x}) = \frac{T}{V_{\text{Block}}} \int_V \mathrm{d}^3 y \, U(\mathbf{x}, \mathbf{y}) W(\mathbf{y}) U(\mathbf{y}, \mathbf{x}), \tag{4.1}$$

where the integration goes over the volume $\sim T^{-3}$ of the block, $U(\mathbf{x}, \mathbf{y})$ is a Wilson line connecting the points $\mathbf{x}$ and $\mathbf{y}$, and $W(\mathbf{x})$ is the temporal Wilson loop. Spatial gauge fields connect adjacent centers of the blocks. The specific details of the blocking volume and the paths of the Wilson lines parallel transporting thermal Wilson loop to the center of the block need not be specified as the details affect only scale $\sim T$ physics, which is outside the domain of validity of the effective theory.

For SU(2), the blocking procedure of the Wilson line almost preserves unitarity, that is, a sum of SU(2) matrices is an element of SU(2) also, up to a real multiplicative constant. Taking furthermore into account that the exponentiation of a sum of the generators of SU(2) can be written as a linear combination of the very same matrices and the unit matrix, it is possible to parametrize $\mathcal{Z}$ as

$$\mathcal{Z} = \frac{1}{2}\Big\{\Sigma \mathbb{1} + i\Pi_a \sigma_a\Big\} \equiv \frac{1}{2}\Sigma \mathbb{1} + i\Pi, \tag{4.2}$$

with real Σ and Π_a, and with σ_a being Pauli matrices.

We again construct the Lagrangian of the theory including in it all the superrenormalizable operators allowed by the symmetries of the fundamental theory. The (parallel transported) Wilson loops transform in the adjoint representation of the local gauge group, and thus the effective theory is required to remain invariant under

$$\mathcal{Z}(\mathbf{x}) \to \Omega(\mathbf{x}) \mathcal{Z}(\mathbf{x}) \Omega^{-1}(\mathbf{x}), \tag{4.3}$$

with $\Omega(\mathbf{x}) \in \mathrm{SU}(2)$. Under a global Z(2) transformation, the Wilson loops are in the fundamental representation and thus the action has to remain invariant under

$$\mathcal{Z}(\mathbf{x}) \to -\mathcal{Z}(\mathbf{x}). \tag{4.4}$$

The field Σ is invariant under the local gauge transformation, whereas the field Π transforms in the adjoint representation. Both fields change signs under Z(2).

	C	P	T	Z(N_c)
$\mathcal{Z}$	$\mathcal{Z}^T$	$\mathcal{Z}$	$\mathcal{Z}^\dagger$	$e^{i2\pi/N_c}\mathcal{Z}$
A_i	$-A_i^*$	$-A_i$	$-A_i$	A_i

Table 4.1: The transformations of the fields in the center symmetric theory under the discrete symmetries of the full theory C, P, T, and Z(N_c). The effective theory defined by Eqs. (4.5)-(4.7) is invariant under the discrete symmetries of the full theory.

With these constraints, the most general superrenormalizable action reads

$$S_{\mathrm{Z}(2)} = \int \mathrm{d}^d x\, \mathcal{L}_{\mathrm{Z}(2)}, \tag{4.5}$$

$$\mathcal{L}_{\mathrm{Z}(2)} = g_{\mathrm{Z}}^{-2}\left[\frac{1}{2}\mathrm{Tr}\, F_{ij}^2 + \mathrm{Tr}\,\left(D_i\mathcal{Z}^\dagger D_i\mathcal{Z}\right) + V(\mathcal{Z})\right] \tag{4.6}$$

$$V(\mathcal{Z}) = -p_{\mathrm{Z}} + b_1^{\mathrm{bare}}\Sigma^2 + b_2^{\mathrm{bare}}\Pi_a^2 + c_1\Sigma^4 + c_2(\Pi_a^2)^2 + c_3\Sigma^2\Pi_a^2, \tag{4.7}$$

where the mass terms b_1 and b_2 are additively renormalized by

$$b_1^{\mathrm{bare}} = b_1(\bar{\mu}_{\mathrm{Z}}) + \frac{1}{(4\pi)^2}\left[48c_1^2 + 12c_3^2 + 12c_3 g_{\mathrm{Z}}^2\right]\frac{\mu_{\mathrm{Z}}^{-4\epsilon}}{4\epsilon}, \tag{4.8}$$

$$b_2^{\mathrm{bare}} = b_2(\bar{\mu}_{\mathrm{Z}}) + \frac{1}{(4\pi)^2}\left[80c_2^2 + 4c_3^2 - 40c_2 g_{\mathrm{Z}}^2\right]\frac{\mu_{\mathrm{Z}}^{-4\epsilon}}{4\epsilon}. \tag{4.9}$$

From now on, we will abbreviate $b_i \equiv b_i(\bar{\mu}_{\mathrm{Z}})$. The problem then is to match the coefficients to the full theory. The procedure used in Ref. [3] goes as follows: The phase where $\langle\Pi_a^2\rangle$ is small and $\langle\Sigma\rangle > 0$ is identified with the deconfined phase of the full theory. Here, in the broken phase the fluctuations of the adjoint scalar field around the minimum are then identified as the color electric field of EQCD and the trace of the matrix as the Polyakov loop. As the fluctuations of the Polyakov loop deep in the deconfined phase are small, the mass of the corresponding field will be parametrically heavy, and it is possible to integrate Σ out in perturbation theory resulting in the action of EQCD.

This scale hierarchy is incorporated to the potential by splitting it to two pieces:

$$\begin{aligned} V(\mathcal{Z}) = {} & \left\{h_1\mathrm{Tr}\,(\mathcal{Z}^\dagger\mathcal{Z}) + h_2(\mathrm{Tr}\,\mathcal{Z}^\dagger\mathcal{Z})^2\right\} \\ & + g_{\mathrm{Z}}^2\left\{s_1\mathrm{Tr}\,\Pi^2 + s_2\left(\mathrm{Tr}\,\Pi^2\right)^2 + s_3\Sigma^4\right\}. \end{aligned} \tag{4.10}$$

The former part, the hard potential, is invariant under an extra SU(2)×SU(2) global symmetry

$$\mathcal{Z} \to \Omega_1\mathcal{Z}\Omega_2, \quad \Omega_i \in \mathrm{SU}(2), \tag{4.11}$$

whereas the latter part, the soft potential, breaks the auxiliary symmetry. Thus, the fields proportional to the generators of SU(2) are Goldstone bosons of the hard potential and would remain massless in the absence of the soft potential. However, the soft potential breaks the symmetry and the Goldstone modes acquire a mass squared $\sim g_{\mathrm{Z}}^2$.

To make the above discussion more concrete, consider the one-loop effective potential in the background of the constant classical fields

$$\langle \Sigma \rangle = \rho \tag{4.12}$$
$$\langle \Pi_a \rangle = \omega\, \delta_{a,3}. \tag{4.13}$$

The direction of the latter in color space is arbitrary as it is attainable from any other constant field configuration by a gauge transformation. The one-loop effective potential reads in a general R_ξ gauge

$$\begin{aligned} V_{\rm eff} &= g_{\rm Z}^{-2}\left(b_1\rho^2 + b_2\omega^2 + c_1\rho^4 + c_2\omega^4 + c_3\rho^2\omega^2\right) - \frac{|\omega|^3}{6\pi}\left(2-\xi^{3/2}\right) \\ &- \frac{1}{12\pi}\Big\{\left(b_1+b_2+6\rho^2c_1+6\omega^2c_2+(\rho^2+\omega^2)c_3-\sqrt{\eta}\right)^{3/2} \\ &+ \left(b_1+b_2+6\rho^2c_1+6\omega^2c_2+(\rho^2+\omega^2)c_3+\sqrt{\eta}\right)^{3/2} \\ &+ 2\left(\xi\omega^2+2b_2+4\omega^2c_2+2\rho^2c_3\right)^{3/2}\Big\} + \mathcal{O}(g_{\rm Z}^2), \end{aligned} \tag{4.14}$$

where ξ is the gauge parameter and we have denoted

$$\eta = \left(b_1-b_2+6(\rho^2c_1-\omega^2c_2)-(\rho^2-\omega^2)c_3\right)^2 + 16\rho^2\omega^2c_3^2. \tag{4.15}$$

The first term in Eq. (4.14) is the classical potential, and the rest comes from the fluctuation determinants. Note that the effective potential is not a gauge invariant quantity, it explicitly depends on ξ. This is due to the gauge variant source fields, which force the classical fields to the desired values. However, when the sources are dialed to zero, that is, we are considering minima of the potential, the gauge dependence is lifted.

Looking at the potential order by order in $g_{\rm Z}$, we find at the leading order

$$V_{\rm eff} = \frac{g_{\rm Z}^{-2}}{4}\left(\rho^2+\omega^2\right)\left(2h_1+h_2\left(\rho^2+\omega^2\right)\right) + \mathcal{O}(g_{\rm Z}^0), \tag{4.16}$$

which is clearly minimized by $\rho=\omega=0$ for $h_1>0$. For $h_1<0$ the potential obtains a form of a Mexican hat, with the minimum being located at

$$\rho^2+\omega^2 = v^2 = -\frac{h_1}{h_2} + \mathcal{O}(g_{\rm Z}^2). \tag{4.17}$$

The phase with $h_1<0$ is associated with the deconfined phase of the full theory.

Parametrizing the field in the leading order minimum of the potential as

$$\rho = v\cos(\pi\alpha), \tag{4.18}$$
$$\omega = v\sin(\pi\alpha), \tag{4.19}$$

with a real α, the NLO effects of the the effective potential have the form

$$V_{\rm eff} = \frac{s_1v^2}{2}\sin^2(\pi\alpha) + \frac{s_2v^4}{4}\sin^4(\pi\alpha) + s_3v^4\cos^4(\pi\alpha) - \frac{v^3}{3\pi}\left|\sin(\pi\alpha)\right|^3 + \mathcal{O}(g_{\rm E}^2). \tag{4.20}$$

The locations of the minima of the function $V_{\rm eff}$ in Eq. (4.20) depend on the values of v and s_i. As the theory will be constructed so that it inherits the Z(2) minima structure of the effective potential of the full theory Polyakov loop, the parameter space is restricted

to obtain values such that the potential is minimized at $\alpha = n\pi$, $n \in \mathbb{Z}$. This in turn implies that the effective potential has its minima at $\omega = 0$, or

$$\langle \mathcal{Z} \rangle \;=\; \pm\frac{v}{2}\,\mathbb{1}. \tag{4.21}$$

Specializing to fluctuations around one of these physically equivalent Z(2) minima, the field can be expanded around the minimum as

$$\mathcal{Z} = \pm\Big\{\frac{1}{2}v\mathbb{1} + g_{\rm Z}\Big(\frac{1}{2}\,\phi\mathbb{1} + i\chi\Big)\Big\}. \tag{4.22}$$

Now the theory can be connected to the full theory by matching the fluctuations of the adjoint scalar around the deconfining minimum with the color-electric field, achieved by matching the theory to EQCD, and by imposing the condition that the domain wall profiles stretching between the deconfining minima overlap with the 4d result in the semi-classical approximation. To leading order, this gives

$$b_1 \;=\; -\frac{1}{4}r^2T^2, \tag{4.23}$$

$$b_2 \;=\; -\frac{1}{4}r^2T^2 + 0.441841g^2T^2, \tag{4.24}$$

$$c_1 \;=\; 0.0311994r^2 + 0.0135415g^2, \tag{4.25}$$

$$c_2 \;=\; 0.0311994r^2 + 0.008443432g^2, \tag{4.26}$$

$$c_3 \;=\; 0.0623987r^2, \tag{4.27}$$

$$g_{\rm Z}^2 \;=\; g^2T\,, \tag{4.28}$$

where the parameter $r = \sqrt{2h_2}v/T$ is not fixed by the perturbative matching, and is related to the mass ($m_\phi = rT$) associated with the fluctuations of the auxiliary field ϕ around the deconfining minimum. It is related to the details of how the Wilson line is coarse-grained, and is parametrically of order $\mathcal{O}(1)$.

4.2 Phase diagram of the effective theory

The phase diagram of the theory defined by the action in Eqs. (4.5)-(4.7) and the weak coupling matching in Eqs. (4.23)-(4.28) is studied in Ref. [3]. The matching is exact only in the weak coupling limit, and at non-zero g there are corrections, which increase as the temperature is lowered. Ideally, one would be interested in finding the full phase structure of the theory with general values of its parameters b_i and c_i. However, the high dimensionality of the parameter space makes this a daunting task, and so far investigations have been constrained to parameter values matched at weak coupling.

After the matching in Eqs. (4.23)-(4.28), the effective theory is a function of only two dimensionless numbers, the four-dimensional gauge coupling g and the auxiliary mass parameter r, as well as one energy scale given by the three-dimensional gauge coupling $g_{\rm Z}^2$. In contrast to EQCD, the phase diagram (see Fig. 4.2) of the center symmetric theory closely resembles that of the SU(2) Yang-Mills theory: At all fixed values of r, there are three phases, the two deconfined phases with $\langle\Sigma\rangle \neq 0$ which occur at small g, and the remnant of the confined phase with $\langle\Sigma\rangle = 0$, seen at large g. The confined and deconfined phases are separated by a second order transition, which belongs to the universality class

of 3d-Ising model, the correct universality class of the 4d theory. It is noteworthy that the second-order nature of the phase transition makes the effective description exact at the phase transition point as the screening masses vanish and the scale difference grows infinitely, so that the same set of operators gives an exact description of the physics both at T_c and at asymptotically large temperatures.

The end point of the phase diagram at $r = 0$ can be related to the simple $\lambda\phi^4$ theory. With vanishing r, the color-singlet field Σ totally decouples from the gauge and adjoint scalar fields, resulting in disconnected $\lambda\phi^4$ and SU(2) + adjoint Higgs theories, where the simple scalar theory solely dictates the dynamics of the order parameter. The phase diagram of the $\lambda\phi^4$ theory was determined in Ref. [62], and the critical value of g can be extracted from this result simply by changing the renormalization scale.

Also the large r qualitative behavior can be understood analytically. At large r, the hard potential becomes infinitely strong and the field is constrained to the manifold of the minima of the potential. This results in a non-renormalizable theory of SU(2) matrices, where it is difficult to obtain numerical values in the continuum limit. However, it easy to see that this non-renormalizable theory has a phase transition at some finite value of g, and thus it is expected that the critical curve approaches (an unknown) constant at large r.

The phase diagram can be used to estimate the remaining undetermined parameter of the theory, r, so as to best reproduce the properties of the full theory. The critical temperature of SU(2) Yang-Mills is determined in Ref. [63], in terms of the $\overline{\text{MS}}$ scale

$$\frac{T_c}{\Lambda_{\overline{\text{MS}}}} = 1.23(11). \tag{4.29}$$

Assuming a one-loop running for the coupling constant

$$g^2(\bar{\mu}) = \frac{12\pi^2}{11\ln(\bar{\mu}/\Lambda_{\text{QCD}})}, \tag{4.30}$$

with optimized $\bar{\mu} = 6.74T$ [11], the critical coupling can be estimated

$$g^2(T_c) \approx 5.1. \tag{4.31}$$

By imposing a condition for the effective theory to have the phase transition at the same value of the coupling, the remaining parameter can be fixed to

$$r = 2.6(5). \tag{4.32}$$

From the model-building point of view it is remarkable how the critical coupling is so insensitive to the auxiliary heavy mass parameter r for values that are near the matching condition. There is a physical explanation for this behavior, since the dynamics of phase transition is determined by the long wavelength modes of the system, and the mass parameter r is related to the specific geometry of how the Wilson line is coarse-grained at short wavelengths. Thus, it is natural to expect that the microscopic details do not strongly affect the dynamics of the phase transition. At small values of r, there is an anomaly from this behavior: In this regime, the longest wavelength fluctuations are those related to the hard scale and the scale hierarchy of the potential is violated and no decoupling takes place.

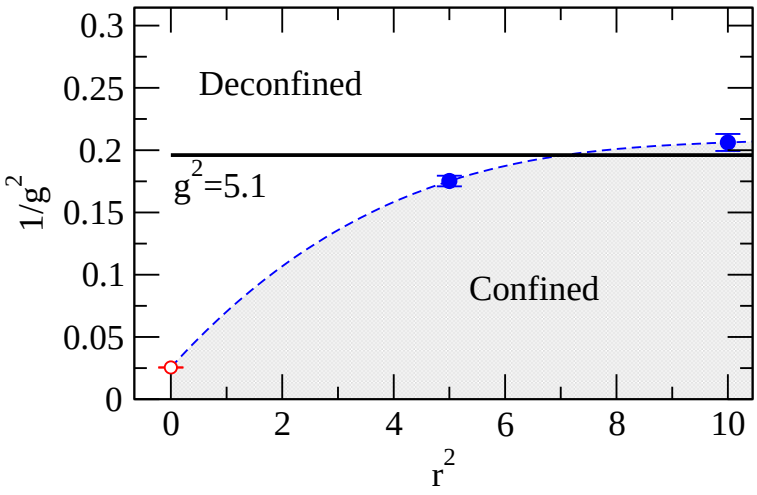

Figure 4.2: The phase diagram of the perturbatively matched center symmetric effective theory on the $(r^2, 1/g^2)$ plane. At all values of the undetermined parameter r, there are confined (at large g) and deconfined (at small g) phases present. At $r = 0$, the curve ends in a point extracted from the $\lambda\phi^4$ theory and approaches a constant at large r^2.

4.3 Center symmetric effective theory for hot SU(3) Yang-Mills theory

A similar approach to construct a center symmetric effective theory for SU(3) Yang-Mills theory was introduced in Ref. [23]. The main difference between the SU(2) and SU(3) cases is that due to the more complex group structure, the coarse-grained Wilson loop is no longer proportional to an element of the group. Rather, the degree of freedom in the SU(3) theory is a general complex matrix. Again for SU(3), the coarse-grained Wilson loop transforms under the adjoint representation of the local gauge group as

$$\mathcal{Z} \to \Omega(\mathbf{x})\mathcal{Z}\Omega^{-1}(\mathbf{x}), \tag{4.33}$$

and the $Z(N_c)$ transformation acts on $\mathcal{Z}$ in the fundamental representation:

$$\mathcal{Z} \to e^{-i2n\pi/3}\mathcal{Z}, \quad n = 1, 2, \ldots \tag{4.34}$$

The set of superrenormalizable operators constructed from the general complex matrix $\mathcal{Z}$ respecting the center symmetry is much larger than in the SU(2) case. On the quartic level, the possible operators are

$$\begin{aligned}
&\mathrm{Tr}\,\mathcal{Z}^\dagger\mathcal{Z}, && \mathrm{Tr}\,\mathcal{Z}\mathrm{Tr}\,\mathcal{Z}^\dagger,\\
&\mathrm{ReTr}\,\mathcal{Z}^3, && \mathrm{ReTr}\,\mathcal{Z}^2\mathrm{Tr}\,\mathcal{Z},\\
&\mathrm{Tr}\,(\mathcal{Z}^\dagger\mathcal{Z}\mathcal{Z}^\dagger\mathcal{Z}), && \mathrm{Tr}\,(\mathcal{Z}^\dagger\mathcal{Z}^\dagger\mathcal{Z}\mathcal{Z}),\\
&\mathrm{Tr}\,\mathcal{Z}^\dagger\mathrm{Tr}\,(\mathcal{Z}^\dagger\mathcal{Z}^2), && \mathrm{Tr}\,\mathcal{Z}\mathrm{Tr}\,(\mathcal{Z}\mathcal{Z}^{\dagger 2}),\\
&\mathrm{Tr}\,(\mathcal{Z}^\dagger\mathcal{Z})\mathrm{Tr}\,(\mathcal{Z}^\dagger\mathcal{Z}), && \mathrm{Tr}\,(\mathcal{Z}^{\dagger 2})\mathrm{Tr}\,(\mathcal{Z}^2).
\end{aligned} \tag{4.35}$$

The large set of operators makes the theory very complicated, with a large number of parameters to match. However, in Ref. [23], it is argued that only a subset of these are

required to capture the essential dynamics of the full theory, and the action in chosen to read

$$S_{\mathrm{Z}(3)} = \int \mathrm{d}^d x \mathcal{L}_{\mathrm{Z}(3)}, \tag{4.36}$$

$$\mathcal{L}_{\mathrm{Z}(3)} = \frac{1}{2}\mathrm{Tr}\, F_{ij}^2 + \mathrm{Tr}\left(D_i \mathcal{Z}^\dagger D_i \mathcal{Z}\right) + V(\mathcal{Z}), \tag{4.37}$$

where the potential consists of two pieces:

$$V(\mathcal{Z}) = -p_{\mathrm{Z}} + V_0(\mathcal{Z}) + V_1(\mathcal{Z}), \tag{4.38}$$

$$V_0(\mathcal{Z}) = c_1^{\mathrm{bare}}\mathrm{Tr}\,[\mathcal{Z}^\dagger\mathcal{Z}] + 2c_2\mathrm{Re}(\det[\mathcal{Z}]) + c_3\mathrm{Tr}\,[(\mathcal{Z}^\dagger\mathcal{Z})^2], \tag{4.39}$$

$$V_1(\mathcal{Z}) = d_1^{\mathrm{bare}}\mathrm{Tr}\,[M^\dagger M] + 2d_2\mathrm{Re}(\mathrm{Tr}\,[M^3]) + d_3\mathrm{Tr}\,[(M^\dagger M)^2], \tag{4.40}$$

with a traceless matrix $M = \mathcal{Z} - \frac{1}{3}\mathrm{Tr}\,[Z]\mathbb{1}$. The first part, V_0, is referred to as the hard potential, and the second part, V_1, as the soft potential in analogy with the SU(2) case. The mass terms c_1^{bare} and d_1^{bare} acquire additive renormalizations in $\overline{\mathrm{MS}}$ renormalization scheme [2]:

$$c_1^{\mathrm{bare}} = c_1(\bar{\mu}_{\mathrm{Z}}) + \frac{1}{16\pi^2}\left[64c_3g_3^2 + \frac{88}{9}c_3^2\right]\frac{\mu_{\mathrm{Z}}^{-\epsilon}}{4\epsilon} \tag{4.41}$$

$$d_1^{\mathrm{bare}} = d_1(\bar{\mu}_{\mathrm{Z}}) + \frac{1}{16\pi^2}\left[\frac{280}{9}c_3^2 - 64d_3g_{\mathrm{Z}}^2 + \frac{92}{3}\left(2d_3c_3 + d_3^2\right) + \frac{9}{2}g_{\mathrm{Z}}^4\right]\frac{\mu_{\mathrm{Z}}^{-\epsilon}}{4\epsilon}. \tag{4.42}$$

The rationale in splitting the fields goes as follows: The hard potential contains three operators, which are invariant under the global SU(3)×SU(3) transformation

$$\mathcal{Z} \to \Omega_1\mathcal{Z}\Omega_2, \quad \Omega_i \in \mathrm{SU}(3), \tag{4.43}$$

and thus depend only on the norm of the matrix. Using a polar decomposition, the part of the matrix affecting the norm can be separated by writing

$$\mathcal{Z} = \lambda\Omega, \tag{4.44}$$

with a complex λ and $\Omega \in \mathrm{SU}(3)$. The idea is then to dial the coefficients of the hard potential, such that it is minimized by a real non-zero λ. In the manifold of the minima of the hard potential, the degree of freedom is proportional to a unitary matrix, appropriate for a coarse-grained Wilson loop. To be explicit, the value of λ minimizing the hard potential is the real root of

$$2c_3\lambda^4 + c_2\lambda^3 + c_1\lambda^2 = 0, \tag{4.45}$$

which is non-zero if $c_2 < 0$ and $c_2^2 > 8c_1c_3$, and corresponds to the global minimum if $c_2^2 > 9c_1c_3$. The hard potential is parametrically stronger than the soft one, and thus the fluctuations representing deviations from unitarity due to coarse-graining will be suppressed by powers of g.

The soft potential breaks the superfluous symmetry and gives rise to the mass and interactions of the color-electric field. The potential is composed of all the superrenormalizable operators which are linearly independent on the manifold of the minima of the hard potential and respect the symmetries of 4d theory. If the fluctuations around the

minimum of the hard potential are small, then the correct dynamics should be captured by this set of operators. The coefficients of the soft potential are dialed such that it is minimized at $M = 0$, that is with $\mathcal{Z}$ proportional to the unit matrix, creating the correct phase structure for the potential.

The effective theory can again be connected to the full theory by integrating out the heavy modes, equating the resulting Lagrangian with EQCD, and matching the domain wall profiles connecting two Z(3) minima in the effective and full theories [23]. At leading order, this gives

$$
\begin{aligned}
c_1 &= \frac{1}{6}\left(m_\chi^2 - 3m_\phi^2\right), && (4.46)\\
c_2 &= -g\frac{m_\chi^2}{\bar{v}T^{1/2}}, && (4.47)\\
c_3 &= g^2\frac{3}{4}\frac{m_\chi^2 + 3m_\phi^2}{\bar{v}^2 T}, && (4.48)\\
d_1 &= g^2T^2, && (4.49)\\
d_2 &= 0.118914g^3T^{3/2}, && (4.50)\\
d_3 &= \frac{3}{4\pi^2}g^4T, && (4.51)\\
g_{\rm Z} &= g^2T, && (4.52)
\end{aligned}
$$

with

$$\bar{v} = 3.005868, \tag{4.53}$$

where instead of one undetermined parameter r, as in SU(2) case, we are left with two undetermined parameters m_ϕ^2 and m_χ^2.

Chapter 5

Conclusions

In this thesis, it has been demonstrated that dimensional reduction provides a powerful tool for the study of quark-gluon plasma even at low temperatures near the deconfinement transition, and can be used to describe the equilibrium thermodynamic properties of the matter created in on-going ultra-relativistic heavy-ion collision experiments. While perturbation theory inevitably fails at these low temperatures due to the non-trivial physics associated with the static long wavelength modes, the physics of the hard modes is still fairly perturbative near T_c. Dimensional reduction provides an elegant framework for analytically integrating out the hard modes, and for dealing with the long wavelength modes using lattice simulations. This setup presents a remedy for the infrared problems of the weak coupling expansion and can be used to pursue high-order contributions unattainable by strictly analytic considerations, though practical computations will require significant progress in the technology of diagrammatic calculations. In Ref. [44], the only input that is not attainable by analytic computations, but is needed for the g^6 term in the weak coupling expansion of the pressure of QCD, was determined by measuring the plaquette expectation value of 3d pure gauge theory. This result was generalized to an arbitrary number of colors in Ref. [1]. However, as the matching between EQCD and QCD has not been performed yet at this level, the full g^6 result still awaits completion.

Lattice simulations in the effective theories are significantly less computer-time consuming than those in the full theory. This is due to the fact that fermions affect the effective theory only through the renormalization of its couplings. This together with superrenormalizability makes it possible to reach a reliably the continuum limit with a moderate computational effort.

Surprisingly, despite the fact that EQCD is constructed to work in the high temperature regime, it still gives a good description of the plasma all the way down to $\sim 2T_c$. At lower temperatures near the transition, the effect of the $\mathrm{Z}(N_\mathrm{c})$ vacua however becomes important for the dynamics of the physical system. In order for a dimensionally reduced theory to accommodate the correct phase structure it must respect all the symmetries of the full theory, which EQCD fails to do as it explicitly violates the center symmetry. To this end, we have constructed and investigated superrenormalizable three-dimensional effective theories for $\mathrm{SU}(N_\mathrm{c})$ Yang-Mills theory that respects the center symmetry as they are formulated in terms of a coarse-grained Wilson loop variable. In the case of SU(2), we have observed a dramatic impact of respecting the symmetries in the phase diagram, where with only leading order perturbative matching, the theory accommodates a phase transition in the correct universality class. Remarkably, this takes place at a value of the

effective theory coupling constant, which is consistent with the value of the full theory coupling at the critical temperature.

Bibliography

[1] A. Hietanen and A. Kurkela, "Plaquette expectation value and lattice free energy of three-dimensional SU(N) gauge theory," JHEP **0611** (2006) 060 [arXiv:hep-lat/0609015].

[2] A. Kurkela, "Framework for non-perturbative analysis of a Z(3)-symmetric effective theory of finite temperature QCD," Phys. Rev. D **76** (2007) 094507 [arXiv:0704.1416 [hep-lat]].

A. Kurkela, "Z(3)-symmetric effective theory of hot QCD," PoS **LAT2007** (2007) 199 [arXiv:0711.1796 [hep-lat]].

[3] Ph. de Forcrand, A. Kurkela and A. Vuorinen, "Center-Symmetric Effective Theory for High-Temperature SU(2) Yang-Mills Theory," arXiv:0801.1566 [hep-ph].

[4] J. Adams *et al.* [STAR Collaboration], "Experimental and theoretical challenges in the search for the quark gluon plasma: The STAR collaboration's critical assessment of the evidence from RHIC collisions," Nucl. Phys. A **757** (2005) 102 [arXiv:nucl-ex/0501009];

K. Adcox *et al.* [PHENIX Collaboration], "Formation of dense partonic matter in relativistic nucleus nucleus collisions at RHIC: Experimental evaluation by the PHENIX collaboration," Nucl. Phys. A **757** (2005) 184 [arXiv:nucl-ex/0410003];

I. Arsene *et al.* [BRAHMS Collaboration], "Quark gluon plasma and color glass condensate at RHIC? The perspective from the BRAHMS experiment," Nucl. Phys. A **757** (2005) 1 [arXiv:nucl-ex/0410020];

B. B. Back *et al.*; "The PHOBOS perspective on discoveries at RHIC," Nucl. Phys. A **757** (2005) 28 [arXiv:nucl-ex/0410022].

[5] L. D. McLerran and B. Svetitsky, "A Monte Carlo Study of SU(2) Yang-Mills Theory at Finite Temperature," Phys. Lett. B **98** (1981) 195.

[6] L. D. McLerran and B. Svetitsky, "Quark Liberation at High Temperature: A Monte Carlo Study of SU(2) Gauge Theory," Phys. Rev. D **24** (1981) 450.

[7] G. Boyd, J. Engels, F. Karsch, E. Laermann, C. Legeland, M. Lütgemeier and B. Petersson, "Thermodynamics of SU(3) Lattice Gauge Theory," Nucl. Phys. **B469** (1996) 419 [arXiv:hep-lat/9602007];

A. Papa, "SU(3) thermodynamics on small lattices," Nucl. Phys. **B478** (1996) 335 [arXiv:hep-lat/9605004];

B. Beinlich, F. Karsch, E. Laermann and A. Peikert, "String tension and thermodynamics with tree level and tadpole improved actions," Eur. Phys. J. **C6** (1999) 133 [arXiv:hep-lat/9707023];

M. Okamoto *et al.* [CP-PACS Collaboration], "Equation of state for pure SU(3) gauge theory with renormalization group improved action," Phys. Rev. **D60** (1999) 094510 [arXiv:hep-lat/9905005];

F. Karsch, "Recent lattice results on finite temerature and density QCD, part II," arXiv:0711.0661 [hep-lat].

[8] Z. Fodor, "QCD Thermodynamics," arXiv:0711.0336 [hep-lat].

[9] E. Braaten and A. Nieto, "Effective field theory approach to high temperature thermodynamics," Phys. Rev. D **51** (1995) 6990 [arXiv:hep-ph/9501375];

E. Braaten and A. Nieto, "Free Energy of QCD at High Temperature," Phys. Rev. D **53** (1996) 3421 [arXiv:hep-ph/9510408].

[10] P. Ginsparg, "First and second order phase transitions in gauge theories at finite temperature," Nucl. Phys. B **170** (1980) 388;

T. Appelquist and R.D. Pisarski, "High-temperature Yang-Mills theories and three-dimensional Quantum Chromodynamics," Phys. Rev. D **23** (1981) 2305.

[11] M. Laine and Y. Schröder, "Two-loop QCD gauge coupling at high temperatures," JHEP **0503** (2005) 067 [arXiv:hep-ph/0503061].

[12] K. Kajantie, M. Laine, K. Rummukainen and M. E. Shaposhnikov, "3d SU(N) + adjoint Higgs theory and finite-temperature QCD," Nucl. Phys. B **503** (1997) 357 [arXiv:hep-ph/9704416].

[13] K. Kajantie, M. Laine, A. Rajantie, K. Rummukainen and M. Tsypin, "The phase diagram of three-dimensional SU(3) + adjoint Higgs theory," JHEP **9811** (1998) 011 [arXiv:hep-lat/9811004].

[14] A. Hart, M. Laine and O. Philipsen, "Static correlation lengths in QCD at high temperatures and finite densities," Nucl. Phys. B **586** (2000) 443 [arXiv:hep-ph/0004060];

A. Hart and O. Philipsen, "The spectrum of the three-dimensional adjoint Higgs model and hot SU(2) gauge theory," Nucl. Phys. B **572** (2000) 243 [arXiv:hep-lat/9908041];

M. Laine and O. Philipsen, "The non-perturbative QCD Debye mass from a Wilson line operator," Phys. Lett. B **459** (1999) 259 [arXiv:hep-lat/9905004].

[15] A. Hietanen and K. Rummukainen, "The diagonal and off-diagonal quark number susceptibility of high temperature and finite density QCD," arXiv:0802.3979 [hep-lat];

A. Hietanen and K. Rummukainen, "Quark number susceptibility of high temperature and finite density QCD," PoS **LAT2007** (2007) 192 [arXiv:0710.5058 [hep-lat]];

A. Hietanen and K. Rummukainen, "Quark number susceptibility at high temperature," PoS **LAT2006** (2006) 137 [arXiv:hep-lat/0610111].

[16] A. Cucchieri, F. Karsch and P. Petreczky, "Screening in hot SU(2) gauge theory and propagators in 3D adjoint Higgs model," Nucl. Phys. Proc. Suppl. **94** (2001) 385 [arXiv:hep-lat/0010023].

[17] K. Kajantie, M. Laine, K. Rummukainen and Y. Schröder, "The pressure of hot QCD up to $g^6 \ln(1/g)$," Phys. Rev. D **67** (2003) 105008 [hep-ph/0211321].

[18] K. Kajantie, M. Laine, K. Rummukainen and M. E. Shaposhnikov, "Generic rules for high temperature dimensional reduction and their application to the standard model," Nucl. Phys. B **458** (1996) 90 [arXiv:hep-ph/9508379].

[19] K. Kajantie, M. Laine, K. Rummukainen and M. E. Shaposhnikov, Phys. Lett. B **423**, (1998) 137 [arXiv:hep-ph/9710538].

[20] A. D. Linde, "Infrared Problem in Thermodynamics of the Yang-Mills Gas," Phys. Lett. B **96** (1980) 289.

[21] G. Endrodi, Z. Fodor, S. D. Katz and K. K. Szabo, "The equation of state at high temperatures from lattice QCD," arXiv:0710.4197 [hep-lat].

[22] C. Torrero, M. Laine, Y. Schröder, F. Di Renzo and V. Miccio, "Towards 4-loop NSPT result for a 3-dimensional condensate-contribution to hot QCD pressure," arXiv:0711.1176 [hep-lat].

[23] A. Vuorinen and L. G. Yaffe, "Z(3)-symmetric effective theory for SU(3) Yang-Mills theory at high temperature," Phys. Rev. D **74** (2006) 025011 [arXiv:hep-ph/0604100]; A. Vuorinen, "Z(3)-symmetric effective theory for pure gauge QCD at high temperature," Nucl. Phys. A **785** (2007) 190 [arXiv:hep-ph/0608162].

[24] J. Engels, J. Fingberg and M. Weber, "Finite size scaling analysis of SU(2) lattice gauge theory in (3+1)-dimensions," Nucl. Phys. B **332** (1990) 737;

A. Velytsky, "Finite temperature SU(2) gauge theory: critical coupling and universality class," arXiv:0711.0748 [hep-lat].

[25] E. Laermann and O. Philipsen, "Status of lattice QCD at finite temperature," Ann. Rev. Nucl. Part. Sci. **53** (2003) 163 [arXiv:hep-ph/0303042].

[26] F. Karsch, E. Laermann and A. Peikert, "The pressure in 2, 2+1 and 3 flavour QCD," Phys. Lett. B **478** (2000) 447 [arXiv:hep-lat/0002003].

[27] R. Hagedorn, "Statistical thermodynamics of strong interactions at high-energies," Nuovo Cim. Suppl. **3**, (1965) 147.

[28] F. Karsch, K. Redlich and A. Tawfik, "Hadron resonance mass spectrum and lattice QCD thermodynamics," Eur. Phys. J. C **29** (2003) 549 [arXiv:hep-ph/0303108];

F. Karsch, K. Redlich and A. Tawfik, "Thermodynamics at non-zero baryon number density: A comparison of lattice and hadron resonance gas model calculations," Phys. Lett. B **571** (2003) 67 [arXiv:hep-ph/0306208].

[29] D. J. Gross and F. Wilczek, "Ultraviolet Behavior of Non-Abelian Gauge Theories," Phys. Rev. Lett. **30** (1973) 1343;

H. D. Politzer, "Reliable Perturbative Results for Strong Interactions?," Phys. Rev. Lett. **30** (1973) 1346.

[30] E. V. Shuryak, "Theory of Hadronic Plasma," Sov. Phys. JETP **47** (1978) 212 [Zh. Eksp. Teor. Fiz. **74** (1978) 408];

S. A. Chin, "Transition to Hot Quark Matter In Relativistic Heavy Ion Collision," Phys. Lett. B **78** (1978) 552;

J. I. Kapusta, "Quantum Chromodynamics at High Temperature," Nucl. Phys. B **148** (1979) 461;

T. Toimela, "The Next Term in the Thermodynamic Potential of QCD," Phys. Lett. B **124** (1983) 407;

P. Arnold and C. X. Zhai, "The Three Loop Free Energy for Pure Gauge QCD," Phys. Rev. D **50** (1994) 7603 [arXiv:hep-ph/9408276];

P. Arnold and C. X. Zhai, "The Three Loop Free Energy for High Temperature QED and QCD With Fermions," Phys. Rev. D **51** (1995) 1906 [arXiv:hep-ph/9410360];

C. X. Zhai and B. Kastening, "The Free energy of hot gauge theories with fermions through g^5," Phys. Rev. D **52** (1995) 7232 [arXiv:hep-ph/9507380].

[31] A. Nieto, "On perturbative QCD at finite temperature," arXiv:hep-ph/9707267.

[32] R. D. Pisarski, "Fuzzy bags and Wilson lines," Prog. Theor. Phys. Suppl. **168** (2007) 276 [arXiv:hep-ph/0612191].

[33] M. Cheng *et al.*, "The QCD Equation of State with almost Physical Quark Masses," arXiv:0710.0354 [hep-lat].

[34] K. Kajantie, T. Tahkokallio and J. T. Yee, "Thermodynamics of AdS/QCD," JHEP **0701** (2007) 019 [arXiv:hep-ph/0609254].

[35] P. H. Ginsparg and K. G. Wilson, "A Remnant of Chiral Symmetry on the Lattice," Phys. Rev. D **25** (1982) 2649;

[36] O. Kaczmarek, F. Karsch, P. Petreczky and F. Zantow, "Heavy quark anti-quark free energy and the renormalized Polyakov loop," Phys. Lett. B **543** (2002) 41 [arXiv:hep-lat/0207002].

[37] D.J. Gross, R.D. Pisarski and L.G. Yaffe, "QCD and instantons at finite temperature," Rev. Mod. Phys. **53** (1981) 43.

[38] T. Bhattacharya, A. Gocksch, C. Korthals Altes and R. D. Pisarski, "Interface tension in an SU(N) gauge theory at high temperature," Phys. Rev. Lett. **66** (1991) 998.

[39] N. Weiss, "The Effective Potential for the Order Parameter of Gauge Theories at Finite Temperature," Phys. Rev. D **24** (1981) 475.

[40] N. Weiss, "The Wilson Line in Finite Temperature Gauge Theories," Phys. Rev. D **25** (1982) 2667.

[41] T. Appelquist and J. Carazzone, Phys. Rev. D **11** (1975) 2856.

[42] S. Chapman, Phys. Rev. D **50** (1994) 5308 [arXiv:hep-ph/9407313].

[43] S. Kratochvila and P. De Forcrand, "Testing dimensional reduction in SU(2) gauge theory," Nucl. Phys. Proc. Suppl. **106** (2002) 522 [arXiv:hep-lat/0110138].

[44] A. Hietanen, K. Kajantie, M. Laine, K. Rummukainen and Y. Schröder, "Plaquette expectation value and gluon condensate in three dimensions," JHEP **0501** (2005) 013 [arXiv:hep-lat/0412008];

A. Hietanen, K. Kajantie, M. Laine, K. Rummukainen and Y. Schröder, "Non-perturbative plaquette in 3d pure SU(3)," PoS **LAT2005** (2006) 174 [arXiv:hep-lat/0509107].

[45] C. P. Korthals Altes, R. D. Pisarski and A. Sinkovics, "The potential for the phase of the Wilson line at nonzero quark density," Phys. Rev. D **61** (2000) 056007 [arXiv:hep-ph/9904305].

[46] M. Laine and A. Rajantie, "Lattice-continuum relations for 3d SU(N)+Higgs theories," Nucl. Phys. B **513** (1998) 471 [arXiv:hep-lat/9705003].

[47] K. Kajantie, M. Laine, K. Rummukainen and Y. Schröder, "Four-loop vacuum energy density of the SU($N_{\rm c}$) + adjoint Higgs theory," JHEP **0304** (2003) 036 [arXiv:hep-ph/0304048].

[48] S. Nadkarni, "Dimensional Reduction in Finite Temperature Quantum Chromodynamics. 2," Phys. Rev. D **38** (1988) 3287.

[49] A. Gynther, M. Laine, Y. Schröder, C. Torrero and A. Vuorinen, "Four-loop pressure of massless O(N) scalar field theory," JHEP **0704** (2007) 094 [arXiv:hep-ph/0703307].

[50] S. Bronoff and C. P. Korthals Altes, "Phase diagram of 3D SU(3) gauge-adjoint Higgs system and C-violation in hot QCD," Phys. Lett. B **448** (1999) 85 [arXiv:hep-ph/9811243].

[51] A. Rajantie, Nucl. Phys. B **501** (1997) 521 [arXiv:hep-ph/9702255].

[52] S. Bronoff, R. Buffa and C. P. Korthals Altes, "Phase diagram of 3D SU(3) gauge-adjoint Higgs system," arXiv:hep-ph/9809452.

[53] H. Panagopoulos, A. Skouroupathis and A. Tsapalis, "Free energy and plaquette expectation value for gluons on the lattice, in three dimensions," Phys. Rev. D **73** (2006) 054511 [arXiv:hep-lat/0601009].

[54] U. M. Heller and F. Karsch, "One Loop Perturbative Calculation of Wilson Loops on Finite Lattices," Nucl. Phys. B **251** (1985) 254.

[55] F. Di Renzo, M. Laine, V. Miccio, Y. Schröder and C. Torrero, "The leading non-perturbative coefficient in the weak-coupling expansion of hot QCD pressure," JHEP **0607** (2006) 026 [arXiv:hep-ph/0605042].

[56] M. J. Teper, "SU(N) gauge theories in 2+1 dimensions," Phys. Rev. D **59** (1999) 014512 [arXiv:hep-lat/9804008].

[57] B. Lucini and M. Teper, "SU(N) gauge theories in 2+1 dimensions: Further results," Phys. Rev. D **66** (2002) 097502 [arXiv:hep-lat/0206027].

[58] G. 't Hooft, "A planar diagram theory for strong interactions" Nucl. Phys. B **72** (1974) 461.

[59] S. Datta and S. Gupta, "Dimensional reduction and screening masses in pure gauge theories at finite temperature," Nucl. Phys. B **534** (1998) 392 [arXiv:hep-lat/9806034].

[60] S. Datta and S. Gupta, "Screening masses in SU(2) pure gauge theory," Phys. Lett. B **471** (2000) 382 [arXiv:hep-lat/9906023].

[61] R. D. Pisarski, "Quark-gluon plasma as a condensate of SU(3) Wilson lines," Phys. Rev. D **62** (2000) 111501 [arXiv:hep-ph/0006205];

A. Dumitru and D. Smith, "Eigenvalue repulsion in an effective theory of SU(2) Wilson lines in three dimensions," arXiv:0711.0868 [hep-lat].

[62] X. P. Sun, "Monte Carlo studies of three-dimensional O(1) and O(4) phi**4 theory related to BEC phase transition temperatures," Phys. Rev. E **67** (2003) 066702 [arXiv:hep-lat/0209144].

[63] J. Fingberg, U. M. Heller and F. Karsch, "Scaling and Asymptotic Scaling in the SU(2) Gauge Theory," Nucl. Phys. B **392** (1993) 493 [arXiv:hep-lat/9208012].